5. Introduction

Viral vectors, in contrast to non-viral vectors, are far more capable of cellular transfection but their immune response compromise their in *vivo* use (1). Even though its less efficiency, specifically *in vivo*, lipoplex, consisting of a complex of nucleic acids and cationic lipids, is considered to be immunologically safe, and non-toxic than viral vectors for *in vivo* applications. As they are also comparatively easy to formulate and modified chemically to improve transfection efficiency, research in this specific area have been significantly increased in last few years. Several nano careers containing positive charge have been synthesized and structurally improvised in an organised manner to relate structure with transfection activity (2). In addition, performance of these non-viral nano careers might also be optimized by ligand targeting to particular cell types (cancer cells) or to particular region (CNS).

From the time, (N-[1-(2,3,-dioleyloxy)propyl]-N,N,N-trimethylamonium chloride) (DOTMA) was introduced as gene carrier in 1987, liposomes have been maximum studied as non-viral vector for gene delivery (3). Later on, a number of other cationic lipids have been synthesized and tried. Most of cationic lipids possess a hydrophobic group, which may be consisted of single or double fatty acid chains or an alkyl moiety comprised of 12-18 carbons in length and an amine group/groups. The cationic lipids assemble into bilayer vesicles owing to its hydrophobic tails when dispersed in aqueous media and in this process effectively uncovering the amine groups headed for the aqueous medium while protecting the hydrophobic portion. Furthermore, the amine group is a necessity for the transfection efficiency of these vectors, as this group is positively charged at physiological pH and interacts electrostatically with the negatively charged phosphate groups of DNA which is condensed into large anionic molecule and forms small vesicular units – lipoplexes (4). The transfection efficiency of positively charged lipoplexes was originally associated with direct fusion with plasma membrane, however it is now believed that transfection occurs mainly *via* endocytosis. Various factors may affect the stability, formation and DNA transfer capability of lipoplexes such as particle size, zeta potential, and DNA/liposome ratio (L/P ratio). Furthermore, not all cationic lipid molecules can form lipoplexes with DNA by themselves, and are frequently accompanying with neutral lipids or cholesterol.

Novel cationic lipoplexes used in the experiments involve cationic liposomes formed with unrelated neutral lipids phosphatidylcholine (PC), phosphatidylethanolamine (PE) and cholesterol, altogether with synthesised cationic lipids that is developed from modification of DOPE with alkaline amino acids. The molecular structures of HSPC and DPPE are shown

in figure 5.1., were obtained as gift sample from Lipoid AG (Steinhausen / ZG Switzerland), and cholesterol was purchased from Sigma-Aldrich (St. Louis, MO, USA).

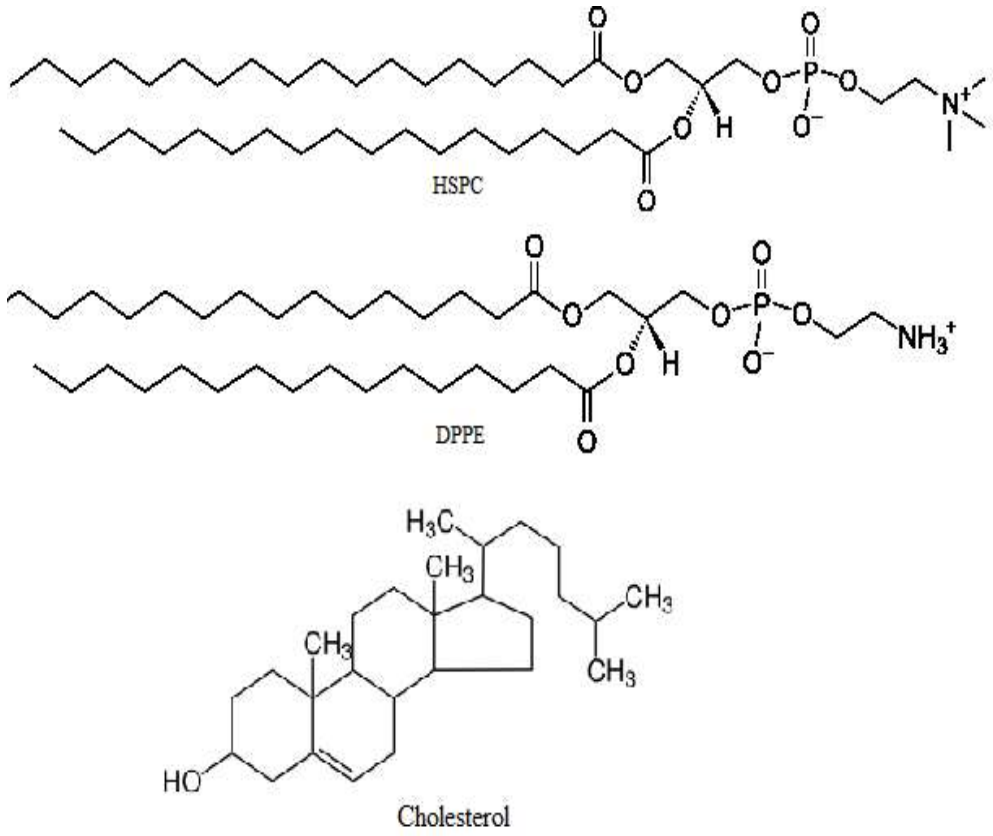

Figure 5. 1 Structures of HSPC, DPPE and Cholesterol

5.1 Preparation of liposomes

The lipid stock solutions were obtained by dissolving the all lipids (HSPC, DPPE, Cholesterol, and modified DOPE) in molar ratio of 5.5: 1: 1.5: 2 in chloroform and methanol (3:1 v/v) mixture in a 50 mL RBF. Additionally, 1 mole % of PEG $_{2000}$-DSPE was added for PEGylation of liposomes. The solvents methanol and chloroform were then evaporated by using a vacuum rotary evaporator system (IKA RV-10, USA) at at -400 to -500 mmHG vacuum and 45–50 °C temperature, at 120 RPM to form a thin lipid film on the wall of RBF. Thin film thus formed was hydrated with DNAse free water-DFW at 65°C temperature and subsequently, formed liposomes were extruded through each of 1 µ, 0.8 µ, 0.4 µ, 0.2 µ, and 0.1 µ polycarbonate membranes (Whatman, USA) supported by polyethylene drain disk (Whatman, USA) using high pressure extruder (Avestin, USA) for 5-7 cycles (5).

For formulation development, different molar ratios of lipids were randomly tried based on prior experience to attain desired particle size distribution. Optimized ratio was used for preparation of liposomes with other lipids synthesized from modifications of DOPE.

5.1.2 Optimization of process parameters

Different process parameters involved in the preparation of liposomes were optimized initially. These process parameters included solvent evaporation time, hydration time and rotation speed of RBF during hydration were optimized for desired results. While keeping other factors constant, effect of one variable was observed on desired output parameters. Results observed are shown in table 5.1.

Table 5. 1 Effects of various process parameters on lipids film and subsequently on liposome formation

Solvent system	
Solvent system	Observation
Chloroform:methanol (1:1 v/v)	Not much suitable for the lipids used for liposome preparation + synthesised lipid containing amino acid headgroup resulting in need of more amount of solvents to get solubilised
Chloroform:methanol (2:1 v/v)	Not much suitable for the lipids used for liposome preparation + synthesised lipid containing amino acid headgroup resulting in more amount of solvent was needed to solubilize all the lipids
Chloroform:methanol (3:1 v/v)	Suitable for all the lipids, Less solvent was needed to solubilize them
Solvent evaporation temperature	
Temperature	Observation
30°C	Not suitable to evaporate solvent system, more time needed for evaporation resulting film varied in thickness, consequently wide-ranged liposomal size distribution obtained
45°C	Suitable for evaporation of solvent mixture under reduced pressure resulting in lowering of boiling point of solvent system
60°C	No further improvement
Solvent evaporation time	
Time (min)	Observation
30	Efficient drying, no smell of residual solvent
60	No further improvements

90	No further improvements
Vacuum condition	
Vacuum (mmHg)	Observation
250	Inefficient drying (more time required)
350	Inefficient drying (more time required)
450	Thin uniform film
Rotation speed	
Rotation speed (RPM)	Observation
75	Localised deposits on the wall with uneven film thickness
100	Thin uniform film
125	Thin uniform film
150	Variable film thickness with breaches in between
Hydration Temperature	
Temperature	Observation
30°C	Inefficient hydration of lipid film, non-hydrated spots were observed even after a long period
45°C	Efficient hydration but long time required
60°C	Complete hydration of film
Hydration time	
Time (min)	Observation
60	Many non-hydrated spots were evident in RBF
90	Complete hydration of film
120	Complete hydration of film

5.1.3 Optimization of formulation parameters

In general, DoE is a concept that uses a desired set of experiments to optimize or investigate a studied object. Liposomal formulation was optimized for size and PDI using D-optimal design with total 19 runs among which 6 model points were for preselected quadratic model, 5 points to estimate the lack of fit, 5 replicate points and additional 3 center points to evaluate for curvature and to estimate the pure error. From the results of optimum batch observed in preliminiary screening, molar ratio of modified DOPE was kept constant i.e. 20 mole % and mPEG 2000 -DSPE level of 1 mole % in experimental design for all batches while varying the mole% of other lipids i.e. HSPC, DPPE and Cholesterol. Chosen variables

for optimization; coded and actual values for optimization are tabulated here in table 5.2 and 5.3 respectively. Furthermore, the design was also constrained as depicted in table 5.4, so as to retain total molar concentration of three chosen lipids to be 80 mole % in each combinations. Additionally, process related parameters were also kept constant throughout the optimization process.

Table 5. 2 Variables and response parameters for design optimization of liposome formulation

Variables	HSPC Cholesterol DPPE
Response parameter	Particle size (nm) PDI

Table 5. 3 Actual and coded values for optimization parameters

Component	Name	Units	Type	Low Actual	High Actual	Low Coded	High Coded
A	HSPC	mole %	Mixture	50	65	0	1
B	Cholesterol	mole %	Mixture	5	17.5	0	0.833333
C	DPPE	mole %	Mixture	10	20	0	0.666667

Table 5. 4 Constrains applied to design for optimization

Design constrains		
Low	**Constraint**	**High**
50	A:HSPC	65
5	B:Cholesterol	17.5
10	C:DPPE	20
	A+B+C	80

5.2 Preparation of Lipoplex

Formulation and process parameters involved in the complexation of cDNA with cationic liposomes were also optimized. The cDNA was added to the diluted cationic liposomes and

the samples were vortexed and maintained at room temperature for 30 minutes to promote the cDNA association with the cationic liposomes (6). Different L/P ratios (ratio of moles of cationic lipid to moles of phosphates of cDNA) were prepared by adding increasing concentrations of 5 µL cDNA solution to 20 µL of cationic liposomes to optimise the maximum complexation efficiency of liposomes.

5.2.1 Optimization of process parameters

Diverse process parameters concerned in the preparation of lipoplexes were optimized primarily. These process parameters included incubation temperature and pH. Retardation of comprehensive quantity of cDNA on gel by lipoplexes was considered as optimum process parameter. While retaining one factor persistent, outcome of alternative variables was observed.

5.3 Physicochemical characterization

5.3.1 Size and zeta potential measurements with dynamic light scattering

One of the most repeatedly stated factors that are accountable for a range of biological effects of nano system are particle size and zeta potential. Dynamic Light Scattering (DLS), commonly recognised as Photon Correlation Spectroscopy or Quasi-Elastic Light Scattering, is a widespread tool within the pharmacy community. DLS is non-invasive, necessitates nominal sample preparation and no calibration. A range of light scattering instruments such as Malvern Zetasizer series, Brookhaven NanoDLS series, and Microtrac Wave II series have appeared in recent years. The size and zeta potential of the cationic liposomes were measured by dynamic light scattering (DLS) by using a Zetasizer NanoZS instrument (Malvern Instruments, Malvern, Worcestershire, UK).

The most frequently used technique to ascertain the electrophoretic mobility of particles is light scattering. Malvern Zetasizer® Nano instruments use laser Doppler electrophoresis to measure small frequency shifts in the scattered light that are proportional to the speed of the particles. In this technique, the laser beam is split into two, one beam is the reference, and the other one is directed towards the sample. The Doppler shift is determined when the scattered light from the sample optically interferes with the reference beam. As the laser beam has to pass through the sample, the sample must be optically clear.

The DLS measurements were performed at 25 °C. When size measurement was performed, the equilibration time was 120 seconds, the scattering angle was 173° and 3 measurements per sample were carried out. The zeta potential measurements were analyzed according to the Smoluchowski model and the equilibration time was set to 120 seconds

5.3.2 Cryo-Transmission Electron Microscopy (Cryo-TEM)

Cryo-TEM is a desired Technique for imaging of liposome in their integral state. The sample was diluted with double amount of water and then 20 ml of sample was applied on suitable Carbon grid whose exterior surface was modified for suitable adhesion of liposomal formulation to the grid surface. Then after, liquid ethane was used to form a thin film of sample using amorphous ice. Subsequently, the grid was conveyed to cryo holder previously upheld at cryo temperature and observed for morphology and lamellarity using Tecnai G2 cryo-TEM (7).

5.3.3 Complexation efficiency

EtBr intercalation assay

Lipoplexes prepared by incubating cDNA with cationic liposomes were subjected for determination of complexation efficiency of cationic liposomes with netatively charged cDNA. Prepared lipoplexes, diluted if necessary, were loaded on to gel using gel loading buffer and electrophoresis was carried out at 5 V/cm for 30 min in 1X TAE buffer. Uncomplexed cDNA migrated on gel was visualized by UV transillumination on GelDoc ImageXR+ system (Bio-Rad Labs., USA). Amount of free cDNA was quantified using DNA calibration curve (8).

Protocol for EtBr assay

Preparation of the Gel

1 % of agarose in a gel was used for the separation of DNA, with most gel ranging between 0.5-2.0 percent depending on the size of the DNA fragments to be separated. TAE as running buffer was added to the agarose containing flask and it was then swirled to mix. Agarose/buffer mixture was melted in microwave for 30 min for agarose to completely dissolve. 0.5 µg/mL concentration of EtBr was added to the melted agarose/buffer mixture. Pour the molten agarose into the gel mould and allow the agarose to set at room temperature. Comb was removed once gel was settled and place the gel in box.

DNA separation procedure

0.25% bromophenol blue was added as loading dye to the DNA samples to be separated. Loading dye assists in trailing how far the DNA sample has moved, and also allows the sample to sink into the gel. Power supply of 5 V/cm was programmed and adequate running buffer was added to cover the surface of gel. It is significant to use the identical running buffer as the one used to fix the gel. Power supply was turned on after attaching the leads to the gel box. Samples containing cDNA were then loaded to the well and it was run until the gel has migrated to an appropriate distance.

Observation of separated DNA

When electrophoresis has completed, power supply was turned off and lid of the gel box was removed. Gel was removed from the gel box. Additional buffer was drained off from the gel surface. Gel was placed on tissue paper to absorb any extra running buffer. Gel was exposed to UV light by using a gel documentation system to obtain fluorescent DNA bands.

5.3.4 UV spectrophotometric determination

Lipoplex containing cDNA was sampled in Beckman® ultracentrifugation tubes and centrifuged at 40, 000 RPM for 2 hr at 4°C (OptimaTM Max-xp Ultra Centrifuge; Beckman Coulter, USA). Supernatant was removed and pellet was dispersed by sonication in 100 µL of DFW. 200 µL of phenol/chloroform (1:1) mixture was added and vortexed for vigorous mixing to separate lipids from cDNA. Aqueous layer was separated, washed again with chloroform and subsequent clear phase separation was achieved by centrifugation to eradicate any traces of phenol (9). Washed aqueous layer was separated for spectrophotometric analysis using NanoDrop 2000 instrument (NanoDrop, Germany).

5.4 Stability challenge studies

5.4.1 Electrolyte induced flocculation study

Electrolyte flocculation study was done to evaluate steric stability of prepared lipoplex by estimating extent of steric barrier present around liposomes. Steric stabilization occurs due to the presence of steric barriers from the adsorbed nonionic molecules on particles that prevent the particles from coming close enough to allow van der Waals attractive forces between the particles to dominate (10). The liposomal formulations are predominantly electrostatically stabilized. Addition of electrolyte will compress the electrostatic double layer surrounding the liposomes and results in aggregation followed by flocculation with a corresponding increase in

Optical turbidity.

For the proposed study, lipoplex formulations were dispersed in 1 ml PBS and diluted such that final lipid concentration of 1 mg/ ml was obtained. From this dispersion, 1 ml of aliquot was mixed with 1 ml of sodium sulphate solution of various concentrations ranging from 0 to 5% prepared in 16.7% sucrose solution. The resultant dispersions were mixed carefully and absorbance was measured for all the concentrations within the duration of 5 min at 400 nm on UV–visible spectrophotometer against respective blank solutions. This was additionally confirmed by measuring the size of the liposomes by Zetasizer (11).

5.4.2 Heparin polyanion competition assay

This assay was used to evaluate the stability of cDNA lipoplexes *in vivo* and to confirm that cDNA forms stable complexes with cationic liposomes which are resistant to decomplexation by polyanions like sulphated glaycosaminoglycans found inside body. The formulations were exposed to varying weight ratio of heparin sodium to cDNA (1:1 to 1:4 w/w) and resulting dispersions were incubated for 30 min at room temperature. After incubation, the amount of cDNA decomplexed from liposomes were evaluated using gel electrophoresis (12).

5.4.3 Serum stability study

Detrimental interaction with serum components is one of the major barriers which intravenous nonviral gene delivery has to overcome. Presence of serum leads liposomes to aggregate and further interactions led to lipoplex dissociation, release of DNA and degradation (13). Ability of liposomes to protect cDNA from serum nucleases was evaluated in presence of serum. Naked DNA solution and lipoplex formulations were incubated with 50 µL of FBS keeping constant cDNA concentration for all samples, and final volume was kept so as to give serum concentration of 50% *v/v*. All samples were incubated at 37°C. After incubation, samples were mixed properly with 100 µL of phenol/chloroform (1:1 *v/v*) and centrifuged at 14,000 rpm for 10 min at 4°C and was analysed for stability by UV spectrophotometry as method described above (14).

5.5 Biocompatibility studies

5.5.1 Haemolysis study

Hemolytic potential was ascertained to examine compatibility of various formulations with red blood cells and in that way, estimate its safety when used as a carrier for cDNA (15). Briefly, blood sample was gathered from Wistar rats in heparinized microcentrifuge tubes by retro-orbital sinus puncture. Erythrocytes were turned into pallets by centrifugation at 3000 rpm and 5 min and the settled pallet was redispersed in normal saline to achieve 2 % erythrocyte dispersion. Afterward, 1 ml of 2% erythrocyte dispersion was mixed with 1 ml test samples such that final concentration attained was from 1 to 1000 nM on lipid basis which was incubated for 1 h at 37 º C. It was centrifuged at 3000 rpm for 5 min and supernatant was estimated for free hemoglobin content by determining absorbance at 545 nm using UV–Visible spectrometry using normal saline treatment as negative control and DOTAP containing formulation as positive control (16).

5.5.2 Erythrocyte aggregation study

Cationic lipids are known to induce erythrocyte aggregation and this study can be used to evaluate biocompatibility of lipoplex formulated from synthesised cationic lipids (17). Therefore, erythrocyte aggregation study using rat blood cells was performed. The erythrocyte suspension was prepared by the same protocol as that in haemolysis study. 500 µL 2% erythrocyte suspension containing lipids at different concentrations in lipoplex form was mixed thoroughly by vortexing and incubated for 2 h at 37 ºC. The erythrocyte aggregation was visualised using inverted microscope (18).

5.6 *In vitro* cell line studies

With the arrival of various drug delivery systems like micelles, emulsions, nanoparticles, NLC and liposomes for the treatment, there's been increase in the toxicological assessment of such formulations. This toxicological assessment has also been transformed from *in vivo* to *in vitro* estimation which has arranged for improved and quick outcomes on possibly new chemicals before they can be experienced and used in animals or humans. *In vitro* cell line study is an impending tool that offers an understanding about the clinical relevance of formulations in various conditions. Therefore, *in vitro* assessment has been used since long as a substitute to *in-vivo* assessment owing to their close correlation (19). This, *in vitro* toxicity study is the systematic investigation of the effects of toxic chemical entities on cultured cells. Of all methods the most popular ones are the MTT and XTT dye (tetrazole dyes) based assay methods due to their ease, sensitivity and scalability (20). Here in present investigation, MTT based cytotoxicity assay was used to evaluate cytotoxicity of the lipoplex formulations developed for delivery of p11 gene on SHSY5Y cells.

The MTT assay is one subtle and dependable indicator study related to mitochondrial activity and is favoured over the other studies that measure ATP and ^{3}H-thymidine incorporation assay as an end point, the latter using radioactivity. The assay particularly depend on the reduction of MTT by mitochondrial dehydrogenases to formazan crystal which is water insoluble and purple in colour (21). The formazan crystals are analysed using spectrophotometer (550 nm) after dissolving it in organic solvent. The problem of solubility is resolved by newer generation tetrazolium analogues stabilized by an intermediate electron due to their ability to form water soluble formazan products thus avoiding step to solubilise them in organic solvent such as DMSO. However, the problem was solved but not entirely because the negative charge of these MTT analogues prevent their cellular uptake and may hamper the outcome of the test. Moreover, cell membrane interfering liposomes by its membrane associated electron transport mechanisms affect their reduction. In such cases,

usual dye MTT delivers better opportunity for outcome of toxicity study without hindering any result due to liposomal property or any other mechanisms.

5.6.1 MTT assay

a) Media Preparation

For the preparation of complete media, modified Eagle's medium (MEM) was mixed with 1 % v/v antibiotic solution and 10% v/v fetal bovine serum (FBS), and later on passed through sterile 0.2 µ membrane filter. Screw capped sterile bottles were used for the storage of media. The bottle was then sealed with parafilm and wrapped with aluminum foil. The whole process carried out in vertical laminar air flow cabinet (Weiber Vertical Laminar Air Flow, India).

b) Subculturing of cell line

The SHSY5Y cells obtained from NCCS (pune) were maintained in T-75 cell culture flasks in single layer, and subcultured twice every week by taking 10^4 cells in T-75 flasks. In a humidified atmosphere at 95 % air and 5 % CO2 (Jouan IGO150 CELLlife CO_2 Incubator, Thermo Fisher Scientific, India), they were sub-cultured in complete media stored in sterile bottle at 37°C.

To subculture the cells, following procedures were followed:

- Culture medium was removed from the Tissue culture T-25 flask containing cells and flask was washed with PBS.
- 2 mL of Trypsin-EDTA solution was added to flask and shaken gently to detach the cells from the glass walls and from each other which was observed under the inverted microscope. Removal of Trypsin-EDTA formed the film of cells and it was incubated for 2 minutes for rounding up.
- 5 mL of complete growth medium was added to flask
- Prepared flasks were incubated at 37 C with 5% CO_2 level.

c) Cell Counting Using Haemocytometer

Preparing Haemocytometer:

- 70% IPA was used to clean Haemocytometer.
- The coverslip was attached using moderate pressure and slight circular motions.
- The cell suspension was mixed properly by agitating the flask containing the cells.
- 1 mL of cell suspension was sampled before the cells started settling down.

- Using a micropipette, cells in this sample were gently mixed again to avoid cell lysis. And then 100 µL of sample was pipetted out which was then treated with 100 µl trypan blue with gentle mixing.

Counting**:**

- Some cell suspension comprising trypan blue was drawn out and the haemocytometer was filled cautiously with it.
- 10X objective of the microscope was used to focus grid lines present on the haemocytometer.The number of cells in the area of 16 squares was counted using a hand tally counter. Only live cells that look unstained by trypan blue were counted.
- Counting of cells was continued for all other remaining set of 16 corner squares.
- The haemocytometer is designed so that the number of cells in one set of 16 corner squares is equivalent to the number of cells x 10^4 / mL.
- Calculation of the average no. of cells in 4 sets of 16 corners is as follows: The total count from 4 sets of 16 corners = (Average no. of cells/mL) x 10^4 x 2 Where 10^4 is conversion factor (Conversion of 0.1 mm^3 to mL) and 2 is dilution factor.

d) Preparation of formulation for treatment

- Stock solutions of formulations were sterilized by filtering through 0.2 µ membrane filter. All the dilutions and filtration were carried out in Laminar Air Flow Hood and all the materials and equipment used were sterilized appropriately before use
- Toxicity studies were carried out with the lipoplexes thereof.

MTT assay protocol

The MTT assay (as described above) was used to assess the *in vitro* cytotoxicity of synthesised lipids and lipoplex formulated from these lipids. In brief, SHSY5Y cells (100 µl; 1x10^5 cells/ml) were seeded into 96 well microtitre plates as before and allowed 24 h of time to adhere. Lipoplex formulations in L/P ratio of 2 to 8 (100 µl/well) i.e to be used for MTT assay were diluted in complete media. After 24 h, the medium **was** replaced with filter sterilised complete medium containing lipoplex formulations. The plate was then incubated with formulations for 6 h. Medium was removed after 6 h of incubation with formulations and medium was removed. Cells were washed with freshly prepared PBS and 100 µL of fresh medium containing FBS and antibiotics, was added to each well. After 24 h, 20 µL of 5 mg/ml MTT solution prepared in PBS was added to each well. After incubating for 4 h, the culture medium was removed and 200 µl of DMSO was added. The reduction of viable cells was determined by colorimetry method at 570 nm wavelength using an Enzyme-

Linked Immune Sorbent Assay (21). The number of living cells is directly proportional to the level of the formed formazan, which is quantified in ELISA plate reader.

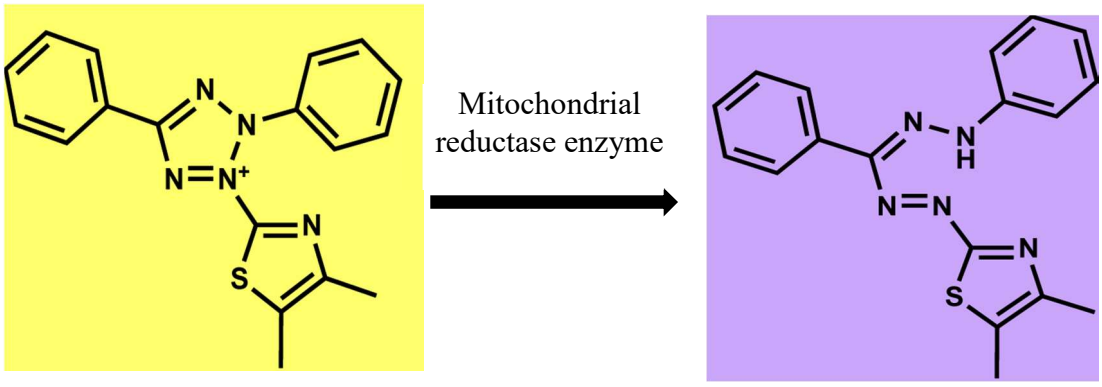

Figure 5. 2 Conversion of MTT to purple coloured Formazan dye

5.6.2 Cellular uptake study

The principle of confocal microscopy is practically well-known one. An objective lens was used to focus light source mostly laser light, on specimen kept on airy disk. The light reflected from the specimen is focused by the same objective lens to a spot on the detector. A pinhole is used to block out of focus planes in a way that only in-spot light will pass and accumulated at detector. By consecutive scanning of planes and a collective use of pin-hole, generates a 3-D image of specimen. Point scanning laser-based systems (confocal laser scanning microscopes, CLSMs) are prevailing for the studies of bacteria or human cell. These typically use galvanometer scanning with a single spot scanning in a raster on the sample. The mixture of monochromatic laser light and profound photomultiplier detector results in exceptional performance in presence of fluorescence which is most abundantly used for working with biological systems. In this system, the image is produced at a very slow speed ($\sim 1 s^{-1}$) which is the limitation of these systems. During the imaging of biological system, higher speeds would be anticipated. This limitation is overcome by availability of various dyes that trace living cells.

The major limitation of the CLSM in biology is its relatively slow acquisition speed (22). When working with living cells, the ability to image fluorescent samples at video speed or higher would be highly desirable. The biological demand for such high-speed systems has been fuelled by an explosion in the availability of dyes for live cell tracing. Vital dyes for specific cell compartments have been used for many years and are now more popular than ever, but two novel approaches have expanded the range of live cell imaging modalities. One type is green fluorescent protein (GFP), originally prepared from genetic modifications

of GFP, others being new isolated from marine organisms. GFP was tagged to plasmid DNA for particular cell component, they can be easily imaged without any hurdle. This expression using GFP can be temporary, bringing together the synthetic gene tagged with GFP into the cell, or long-lasting, by integrating the gene into the genome of a cell line or entire organism (23).

Cellular uptake study protocol

Procedures for media preparation, sub-culturing of cells, cell counting and preparation of formulations were followed as described in the MTT assay earlier. Cells were seeded on cover slip at a density of 5 x 10^4 cells/well which was fixed at the bottom of 6-well plates. Cover slips used were squared shape, 0.17 mm in measurement and flame sterilised on which cells were allowed to grow for 24 h using complete media. After 24 hr, cells were transfected with lipoplexes prepared using optimized liposomal formulations using eGFP at N/P ratio of 2, at a final concentration of 500 ng eGFP pDNA per well. Treatement was carried out for 6 hr and post-treatment, phosphate buffered saline was used to wash the cells. Fresh culture media was added and cells were incubated for 24 hr for expression of eGFP. Cells were washed with PBS followed by treatment with nucleus stain DAPI for 10 minutes followed by washing again with sterile PBS to remove excess DAPI from milieu because excess of DAPI may quench the florescence emitting from eGFP. Coverslips were mounted on sterile glass slides and confocal microscopy was performed on confocal laser scanning microscope (CLSM 710, Carl-Zeiss Inc., USA). Cells treated with naked eGFP pDNA and lipoplexes prepared with Lipofectamine-2000 were used as controls (24).

5.6.3 Cell permeation study

Imitating the *in vitro* responses of blood–brain barrier (BBB) physiologically and functionally is a thought-provoking task. Numerous techniques have been described including an *in silico* model, immobilized artificial membrane chromatography, and a parallel artificial membrane used to foresee drug permeability through particular barrier *in vivo.* In last decade, novel culture techniques and upgraded technologies have delivered the essential tools to produce more convincing *in vitro* cell culture related BBB models to improve our understanding of BBB functionalisation and permeation mechanisms. In last decade, the evaluation of permeability across SHSY5Y single layer of cells turned into one of the prevalent tools for permeation through BBB. Conventional tight junctions can easily polarise SHSY5Y cells (25). Model of BBB contained a porous membrane which separates the upper and lower compartment in a 24-well culture plate which involved two-compartment wells (26). BBB integrity testing is crucial to achieve consistent results of *in*

vitro experiments. Qualitative and quantitative techniques have been developed for the confirmation of the BBB integrity is essential to perform reliable in vitro experiments.

The resistance of tight junctions in BBB models have been comprehensively measured by Transendothelial Electrical Resistance (TEER) measurement. In development of this model, apical membrane cell layer become confluent. Increase in electrical resistance can be seen as increased TEER because of formation of this tight junctions. The tightness of the monolayer is regarded as a quantitative indicator of the resistance for ions to move across BBB layer. [14C] sucrose flux or Lucifer yellow permeability assays have been used for the integrity of *in vitro* human BBB model. However, occasionally use of such compounds melt down the quality of the tested BBB and render them unsuitable for further experiments.

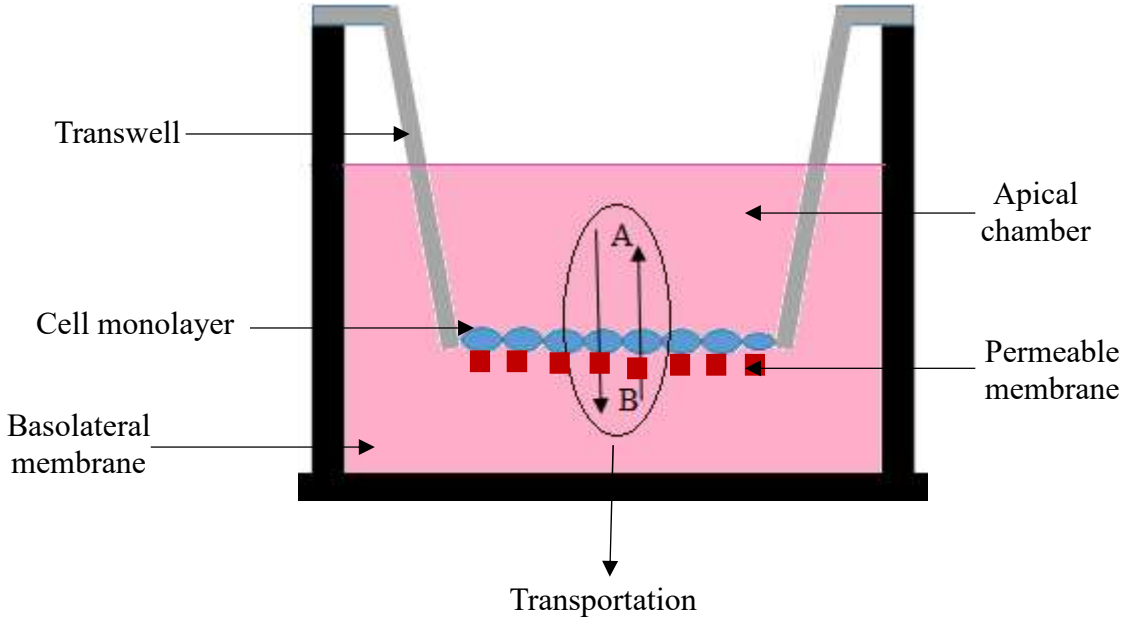

Figure 5. 3 Transwell arrangement for permeation study

Cell permeation study protocol

For the permeation study, SHSY5Y cells adhered to the tissue culture flask, were trypsinised and detached. Later, the cells were seeded in each transwell at density of 1 x 10^6 cells/insert and then 1.5 ml of complete media was added in basolateral chamber. This transwell was then incubated in CO_2 incubator and every day media was changed. Voltohmeter was used to check the monolayer integrity of cells and permeabilty assay was initiated after 91-10 days when TEER (Transepithelial electrical resistance) value above 270 $\Omega.cm^2$ was attained. At the same time, the permeation of Lucifer yellow through the monolayer was measured at the completion of each experiment. The passage of Lucifer yellow through

monolayer was calculated to be < 1 % in all the accompanied experiments. Before starting the experiment, transport media (HBSS + 25mM HEPES + 0.35 g/l $NaHCO_3$) was added to both apical and basal chambers and plate was allowed to equilibrate for 1 h (27). Subsequanlty, p11 cDNA diluted in 1.0 ml transport media and the same, entrapped in modified liposome formulations, were added and plate was incubated at 500 rpm in shaker. 200 µl sample was withdrawn at 15, 30, 60, 90, 120, 180 min and replaced with equal amount of fresh transport media. The samples were analysed by fluorimetry to determine formulation transported to receptor compartment.

5.6.4 Western blot analysis

Main function of Western blot in research is to isolate and identify proteins (28). In western blot analysis, isolation of protein of choice from the cocktail of proteins, is based on molecular weight, using gel electrophoresis. These proteins are then relocated to a membrane fabricating a band for individual protein. This membrane containing protein is then incubated with antibodies specific to the protein of our interest. The antibody in free form (not attached to any protein) is washed off leaving behind only the bound antibody to the protein of interest. The film was developed to detect this antibody. Because of the specificity of antibodies, they only bind to the protein of interest, only one band should be observed. The density of the band relates to the amount of protein present.

a) Lysis buffers

Ability of all lysis buffers differ in their solubilisation capacity of proteins, with those comprising of ionic detergents including sodium dodecyl sulfate (SDS) considered to be strongest and therefore chance are there to give best results. The main criteria for selecting a lysis buffer if they can identify denatured antibody. Tris-HCl buffer was used when the proteins solubilised in cytoplasm.

b) Protease and phosphatase inhibitors

After the lysis process; proteolysis, dephosphorylation and denaturation commences. When the samples are kept in refrigerator at 4°C or on ice, these all aforementioned processes are slowed down and suitable inhibitors are mixed, freshly prepared, to the lysis buffer. These events can be slowed down significantly if samples are kept on ice or at 4°C at all times and appropriate inhibitors are added fresh to the lysis buffer.

c) Preparation of lysate from cell culture

- Petri dish containing cell culture was kept on ice and these cells were washed with ice-cold phosphate buffer saline.

- Remove the PBS, then supplement them with ice-cold lysis buffer.
- Cells were suspended in PBS after two step process of trypsinisation and washing with PBS
- Centrifuge them for 15 min at 10,000 rpm at low temperature after keeping it on continuous agitation at 4°C for half an hr
- Gradually take out the centrifuge tubes from the centrifuge, collect the supernant, keep it on ice and throw away the pellet.
- Absorbance was taken for the protein present in supernant using a spectrophotometer.
- A Bradford assay was performed for the calculation of protein present in supernant and Bovine serum albumin (BSA) is a common protein standard.
- After taking the readings on spectrophotometer, samples were frozen at lowe temperature around -70°C to -80°C for future use and gel loading.

d) Gel preparation

- 10 % stacking gel solution was added with care up to the green bar carrying glass plates with water on top and wait till liquid stacking gel solution solidified, usually for 20-25 min
- Stacking gel was covered with separating gel, after get rid of the top water. Comb was inserted bearing no sign of air bubbles and wait for the gel to get solidified

e) Preparation of samples for loading into gels

- Antibodies usually identify a tiny portion of the protein to be detected (commonly denoted as the epitope) and this portion we talking about may be surrounded by the 3D conformation of the protein of interest. To permit entrance of the antibody to this portion it is essential to unfold the protein by its denaturation
- For denaturation, loading buffer with the anionic detergent sodium dodecyl sulfate (SDS) was used, and boil the blend at 80-90°C for 10 min. Heating at 60-70 °C for 10 -15 min is also suitable. They have tendency to aggregate when boiled or heated and the aggregates formed may not enter the gel matrix competently.
- When anionic surfactant herein, SDS, is used in a ratio of around 1:4 to proteins, proteins acquire negative charge by their affection towards SDS. Denatured proteins attained rod shape with negative charge carrying identical charge densities per unit length. Consequently, movement of protein is only resolute by their molecular weight, but not by the inherent charge present on protein.

- Grade of SDS is also important for quality protein separation. To enable separation by molecular size, 2-mercaptoethanol or dithiothreitol was added to the buffer which reduces disulphide bonds present in proteins. Glycerol was also added to the buffer to increase he density of sample to keep the sample at the bottom of well.
- Bromophenol Blue (an anionic dye small in structure) was added to sample containing loading buffer to visualise migration or movement of proteins. Small structure and anionic nature of dye enable the dye to migrate faster than other component of mixture to be isolated and moreover, it also delivers migration front to display isolation procedure.
- Protein samples should be vortexed, before and after the heating step for the best possible resolution.

f) Electrophoresis

- Gel was placed in electrophorator and running buffer was added to it and power was supplied to electrophorator using electrodes.
- Gel should be entirely deep into buffers and comb was removed with care.
- 6 µL of load maker was added to well containing 15 µL of samples and low voltage of 60 V was applied to run separating gel while for the stacking gel 140 V of higher voltage was applied which was run around for an hr or till the dye does not run off the lowest most part of the gel

g) Electrotransfer

- 6 filter sheets was cut according to measurement of the gel, and also single polyvinylidene fluoride (PDVF) membrane with the identical size.
- Transfer buffer was used to wet the sponge and filter paper whereas methanol was used to wet PDVF membrane
- Glass plates were detached and the gel was retrieved.

Create a transfer sandwich as follows:

- Sponge
- 3 Filter Papers9
- Gel PVDF
- 3 Filter Papers
- Sandwich was transferred to the transfer apparatus

- Transfer apparatus was maintained on ice at low temperature where this prepared sandwich was relocated. This sandwich should be covered with transfer buffer on the top of which electrode was placed

h) Blocking and antibody incubation

- Blocking is a very significant phase of western blotting, as it avoids non-specific antibodies binding to the membrane from binding to the membrane non-specifcally. Blocking is usually accomplished with 5% BSA and nonfat dried milk diluted in TBST which helps reducing background.
- Block the membrane with 5% skim milk in TBST (Tris buffer saline with Tween 20) for almost one hour.
- Primary antibody was mixed in 5% bovine serum albumin (BSA) and incubate for 12 h at 4°C on a shaker (primary antibody was used at a dilution of 1:1000).
- Membrane was washed with TBST for 5 minutes for 3 times.
- Secondary antibody specific for primary antibody was added in 5% skim milk in TBST, and incubate for 1 hour.
- ECL mix was prepared and membrane was incubated with it for a minute, results were visualised in dark room.

Procedure to detect p11 protein

SHSY5Y cells seeded on a 24 well plate at a density of 1,00,000 cells/well were incubated for one day to get 80 % confluency. After incubating for 24 h, already seeded cells were treated with INF-α-2b (interferon), to reduce the p11 protein level (29). After 48 h of incubation, cells were treated with all the modified lipoplex formulations. Cells treated with PBA was taken as negative control. Cells were harvested with trypsin. After washing three times with cold phosphate-buffered saline sterilised by passing through syringe filters of 0.22 μ, cells were resuspended in 50 mM HEPES buffer integrated with complete protease inhibitor and then sonicated three times for 15 s and centrifuged at 12,000 rpm for 15 min. Total protein content was assayed by Bradford method. Ten micrograms of crude cell lysates were separated on Tris-glycine gels and electrophoretically transferred onto a nitrocellulose membrane. p11 protein expression was detected by using 1:1000 dilution of mouse anti-p11 monoclonal antibody (krishgen biotech, Mumbai, India) and 1:3000 dilution peroxidase-conjugated rabbit anti-mouse IgG. The blot was developed using the ECL Western blotting detection system and exposed to radiographic film.

5.6.5 *In vitro* gene expression study by Real time PCR (RT-PCR)

Researchers can study RNA with molecular approach same as for DNA with the help of reverse transcriptase, which has an ability to synthesise DNA from an RNA template (30). PCR uses polymerase chain reaction to amplify cDNA generated by reverse transcriptase. This amplification helps detecting low quantity of RNA present in sample. The very first step of PRC is the denaturation of cDNA by disruption of hydrogen bonds between complementary DNA strands resulting in ssDNA (single stranded DNA) by heating at 95°C. Then for the anneal process to take place, temperature is lowered. This results in annealing of primers complementary to the sequence(s) of interest. Then after DNA synthesis will commence because of DNA polymerase added in the reaction mixture. Now the temperature is raised to 72°C for the DNA polymerase to create new complementary DNA strand. More than this, PCR can selectively amplify DNA template resulting in precise detection of nucleic acid in a specific cell or cell type.

Protocol

In vitro mRNA expression efficiency of different cDNA formulations was evaluated in order to quantify gene expressing potential of lipoplex formulations. RT-PCR was used to quantify mRNA expressed in SHSY5Y cells transfected with different lipoplex formulations. SHSY5Y cells seeded on a 24 well plate at a density of 1,00,000 cells/well were incubated for 24 h to get 80 % confluency. After incubation cells were treated with INF-a-2b (interferon), to reduce the p11 mRNA level. After 48 h of incubation, cells were treated with different lipoplex formulations. Basal gene expression level was evaluated using PBS control i.e. negative control. After another 48 h of incubation, total RNA was isolated using TRIzol reagent and reverse transcriptase into cDNA was carried out using RNA to cdna was carried out using RNA to cDNA conversion kit. mRNA level was quantified using Step One real time PCR using SYBR Green Master mix, forward and reverse primers and lipoplex formulations in a total volume of 10 µL. The mRNA expression level was normalised against housekeeping gene GAPDH.

a) Selection of primer:

- Primers were selected from primer design tool; NCBI (National Center for Biotechnology Information) which is shown in table 5.5
- Primers for mice p11 cDNA were 5’-CAGCCATCTGTTGTTTGCCC-3’ for forward and 5’-CCGCCTCAGAAGCCATAGAG-3’ for reverse (product length 220 bp)

- Primers for mice housekeeping gene GAPDH were 5'-TTATGACCACTGTCCACGCC-3' for forward and 5'-GGCAGGTCAGATCCACAACA-3' for reverse (product length 222 bp)

Table 5. 5 Primer characteristics for mice p11 cDNA and GAPDH gene

Primer	Sequence 5'>3'	Template strand	Length	Start	Stop	Tm
Mice p11 cDNA						
Forward primer	CAGCCATCTGTTGTTTGCCC	Plus	20	1392	1411	60.04
Reverse primer	CCGCCTCAGAAGCCATAGAG	minus	20	1611	1592	59.97
GAPDH housekeeping gene						
Forward primer	TTATGACCACTGTCCACGCC	Plus	20	485	504	60.04
Reverse primer	GGCAGGTCAGATCCACAACA	minus	20	706	687	59.96

b) Lyse samples and separate phases

- 0.4-0.5 mL of TRIzol™ Reagent was added per 1×10^5—10^7 cells directly to the petridish containing cells to lyse them, after removing growth media.
- Centrifuge the lysate at 15,000 × g at 4 °C if sample contains high fat.
- It was then incubated for 10 minutes for the complete detachment of nucleoprotein complex.
- 0.2 ml of $CHCl_3$ was added per 1×10^5—10^7 cells and then tube was capped firmly.
- Tube was incubated for 5 minutes and sample was centrifuged for 10 minutes at 15,000 × g at 4°C. The mixture was separated into 3 layers : lower layer (red coloured phenol-chloroform), a middle phase, and upper water layer.

c) RNA isolation

1. Precipitation and washing of RNA

- Alcohol (IPA) was added in water phase (0.5 ml per 1 mL of TRIzol™).
- Incubate for 10 minutes and centrifuge for 10 minutes at 12,000 × g at 4°C. Total RNA precipitated, forms a white gel-like pellet at the bottom of the tube.
- Supernatant was discarded and RNA was washed.
- For washing of RNA, pellet was suspended again in 80 % ethanol per mL of TRIzol™ Reagent. Sample was centrifuged at 5000 × g at 4°C after vortexing them.
- Supernatant was discarded and precipitated RNA pellet was air dried for 15 minutes.

2. Solubilization of RNA

- Pellet was resuspended in 20–50 µL of RNase-free water and properly mixed with 0.25 mM EDTA, or 0.75 % SDS solution.
- It was then incubated at 65-70 °C for 8-10 minutes.
- RNA samples can be quantified by measuring the absorbance without prior dilution using the NanoDrop™ Spectophotometer and proper dilutions can be achieved to equal the concentration of RNA in each sample.

d) RNA to cDNA conversion

1. Prepare the RT reaction mix

- Before preparing the reaction plate, 20 µL of reaction mix per tube was prepared using components present in kit and it was thawed using ice bath.
- Calculate the volume of components needed to prepare the required number of reactions.

Table 5. 6 Components for RT-PCR reaction

Component	**Volume per reaction**	
	+RT reaction	**-RT reaction**
2X RT Buffer Mix	10.0 µL	10.0 µL
20X RT Enzyme Mix	1.0 µL	-
RNA sample	up to 9 µL	up to 9 µL
Nuclease-free H2O	Q.S.to 20 µL	Q.S.to 20 µL
Total per reaction	20.0 µL	20.0µL

2. Prepare the reverse transcription reactions

- Aliquot 20 µL of RT reaction mix into each well or tube. Seal the plates or tubes. Briefly centrifuge the plate or tubes to spin down the contents and to eliminate any air bubbles.
- Place the plate or tubes on ice until you are ready to load the thermal cycler or Applied Biosystems™ Real-Time PCR system.

3. Perform reverse transcription

- Set the reaction volume to 20 µL. Load the reactions into the thermal cycler or Real-Time PCR system.
- Start the reverse transcription run.

Table 5. 7 RT-PCR temperature cycle

Setting	Step I	step II	Step III
Temperature	37 °C	95°C	4°C
Run	60 minutes	4 minutes	-

4. Store the cDNA

- Store cDNA RT plates or tubes prepared using the High-Capacity RNA-to-cDNA™ Kit for short-term or long-term storage:
- Short-term (up to 24 hours before use)—Store at 2−8°C. Long-term—Store at −25°C to −15°C.
- If required, briefly centrifuge the archive plates or tubes before storing to spin down the contents and to eliminate any air bubbles.

5.7 Result and discussion

The cationic and synthetic lipids were used to provide positive charge to liposomes by conjugating alkaline amino acids (Arginine, lysine and histidine) to DOPE as methods describe in previous chapter. Initially, another lipid, egg phosphatidylcholine, structure of which is shown in figure, was used instead of HSPC. It was chosen in the beginning because a combination of Egg PC and Cholesterol have been used in my previous studies and in several commercial formulations like Myocet® (liposome encapsulated doxorubicin citrate) (31). But in these studies, Egg PC was replaced with HSPC because the liposomes consisting of egg PC and cholesterol were not stable when assembled with cDNA (32). HSPC was chosen because HSPC liposomes have proved to have better DNA carrying ability than Egg PC owing to its stability imparting property.

5.7.1 Formulation optimization using DOE

Response surface modelling was applied using Design Expert 7.0.0. Different polynomial equations were evaluated for best fitting to the experimental data by using multiple linear regression analysis (MLRA) to determine the values of coefficients in the polynomial equations and a full, reduced model was established. Statistical reliability of the established model was assessed by ANOVA statistics. Built on the established model, three-dimensional response surface plots were created by Design Expert Software. The 3D surface plots were convenient in establishing the foremost effects (effect of individual variables) on the response parameter and also to have an understanding of the collective effects of two variables.

Validation of the used experimental design and chosen model for its prediction ability for the optimization of the variables was done by accomplishment of checkpoint analysis. Eight optimum checkpoints were selected, prepared and evaluated for response parameters. Statistical comparison between the predicted values and average of three experimental values of the response parameters was performed to derive percentage error and to evaluate significant difference between these values. Optimum formulation parameters were selected based on the specified goal i.e. particle size and particle size distribution. Optimized formulation was derived by specifying goal and importance to the formulation variables and response parameters. Results obtained from the software are further verified by actual preparation of the batches and comparing the predicted and actual results.

Design matrix

Table 5. 8 Liposome optimization with the help of design matrix

Std	Run	A:HSPC Mole %	B:cholesterol mole %	C:DPPE mole %	Size (nm)	PDI
19	1	54.419	5.581	20.000	225	0.756
16	2	57.623	12.377	10.000	203	0.367
15	3	50.662	9.337	20.000	190	0.245
2	4	54.419	5.580	20.000	231	0.749
9	5	53.764	13.971	12.264	176	0.174
10	6	50.662	9.337	20.000	194	0.546
1	7	60.350	5.000	14.649	211	0.961
13	8	55.564	10.161	14.274	138	0.191
17	9	50.689	17.500	11.810	241	0.387
7	10	55.033	9.7242	15.242	145	0.392
14	11	55.564	10.161	14.274	132	0.199
6	12	50.689	17.500	11.810	225	0.175
12	13	55.564	10.161	14.274	135	0.214
11	14	58.212	8.921	12.865	152	0.531
4	15	57.623	12.377	10.000	160	0.472
3	16	50.000	13.377	16.629	199	0.214
8	17	61.180	8.589	10.230	151	0.364
18	18	64.999	5.001	10.000	203	0.871
5	19	64.999	5.001	10.000	205	0.756

19 batches of liposomes were prepared using composition depicted in the design matrix in table 5.8. All formulations were evaluated for particle size and polydispersity index (PDI) and the results obtained are also shown in table 5.5. All experiments were replicated three times and mean values of experiments were fed to the design matrix for statistical evaluation.

5.7.2 Statistical analysis Response 1 (particle size)

Selection of the predicted model

Summary of the ANOVA results for different models is shown in table 5.9 which portrays sequential p-values and Lack of Fit p-values along with Adjusted and Predicted R-squared values for different models.

Table 5. 9 ANOVA results summary for particle size

Source	Sum of Squares	df	Mean Square	F Value	p-value Prob > F	
Linear	20619.8	9	2291.09	14.5996	0.0009	
Quadratic	1996.57	6	332.761	2.12046	0.1741	
Special Cubic	608.959	5	121.792	0.7761	0.5965	**Suggested**
Cubic	249.355	2	124.678	0.79449	0.4887	
Pure Error	1098.5	7	156.929			

Source	Std. Dev.	R-Squared	Adjusted R-Squared	Predicted R-Squared	PRESS	
Linear	36.8428	0.03675	-0.0837	-0.3712	30916.2	
Quadratic	15.4299	0.86273	0.80993	0.66488	7555.84	
Special Cubic	11.9285	0.92427	0.88641	0.80289	4444.14	**Suggested**
Cubic	12.2377	0.94022	0.88044	0.23292	17295.2	

Highest polynomial displaying highest Lack of Fit p-value 0.5965 i.e.>0.1, was considered for model selection. Based on the criteria special cubic model was found to be best fitted to the observed responses. Quadratic and other models were not suitable for prediction either due to low R-squared values and/or due to higher p value as contrasted to special cubic model which is shown in table 5.10.

Table 5. 10 ANOVA results for special cubic model

Source	Sum of Squares	df	Mean Square	F Value	p-value Prob > F	
Model	20839.5	6	3473.25	24.4099	< 0.0001	**significant**
Linear Mixture	828.641	2	414.32	2.91184	0.0931	
AB	4545.52	1	4545.52	31.9458	0.0001	
AC	70.6306	1	70.6306	0.49639	0.4945	
BC	1902.16	1	1902.16	13.3684	0.0033	
ABC	1387.61	1	1387.61	9.75208	0.0088	
Residual	1707.46	12	142.288			
Lack of Fit	608.959	5	121.792	0.7761	0.5965	**not significant**
Pure Error	1098.5	7	156.929			
Cor Total	22546.9	18				

The Model F-value of 24.099 implies the model is significant. There is only a 0.01 % chance that a "Model F-Value" this large could occur due to noise. Values of "Prob > F" less than 0.0500 indicate model terms are significant. In this case AB, ABC are significant model terms. Values greater than 0.1000 indicate the model terms are not significant. If there are many insignificant model terms (not counting those required to support hierarchy), model reduction may improve model. The "Lack of Fit F-value" of 0.78 implies the Lack of Fit is not significant relative to the pure error. There is a 59.65 % chance that a "Lack of Fit F-value" this large could occur due to noise.

Table 5. 11 Summary of ANOVA result for special cubic model

Std. Dev.	11.93	**R-Squared**	0.9243
Mean	185.05	**Adj R-Squared**	0.8864
C.V. %	6.45	**Pred R-Squared**	0.8029
PRESS	4444.14	**Adeq Precision**	13.529

As shown in table 5.11, the "Pred R-Squared" of 0.8029 is in moderately harmony with the "Adj RSquared" of 0.8864 i.e. <0.2. "Adeq Precision" measures the signal to noise ratio. A ratio greater than 4 is desirable. Consequently, ratio of 13.529 indicates an adequate signal. This model can be used to navigate the design space.

Final Equation in Terms of Actual Components:

size =

-1.94453 * HSPC

-59.57715 * Cholesterol

-43.45504 * DPPE

+1.75590 * HSPC * Cholesterol

+1.23787 * HSPC * DPPE

+13.42311 * Cholesterol * DPPE

-0.30373 * HSPC * Cholesterol * DPPE

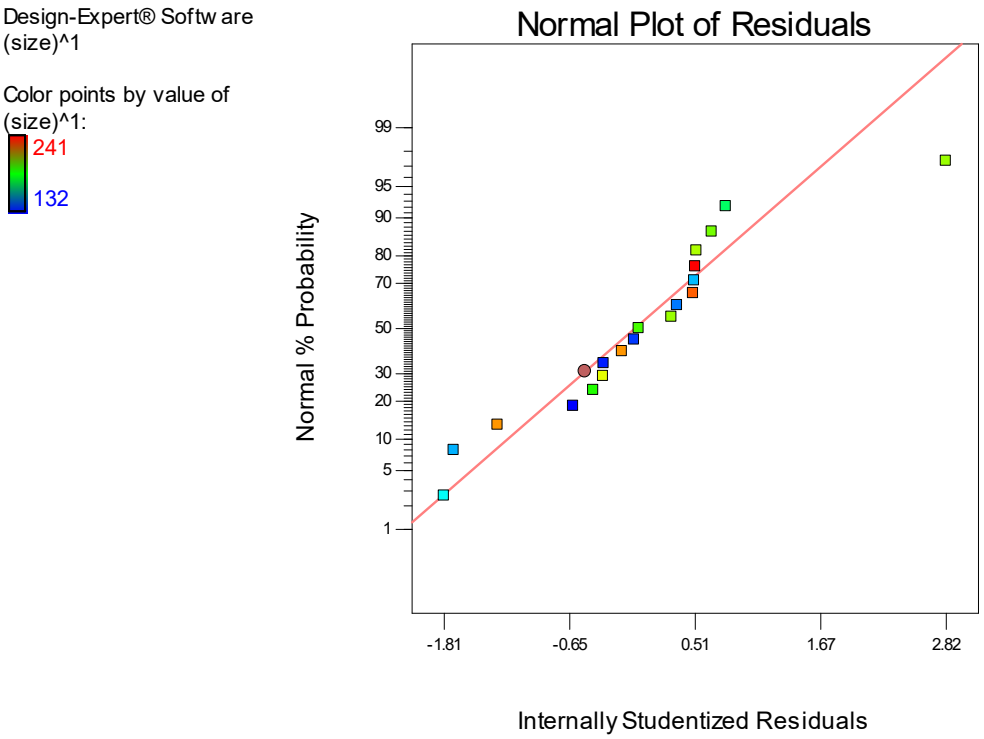

Figure 5. 4 Normal plot of residuals for particle size

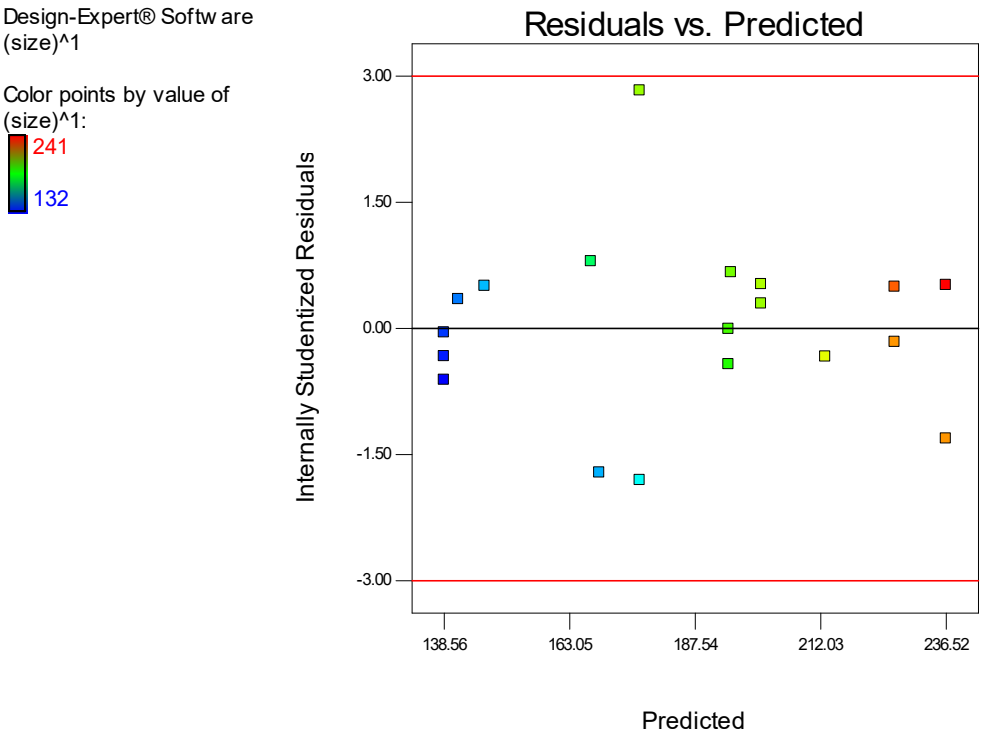

Figure 5. 5 Residuals vs. predicted response plot for particle size

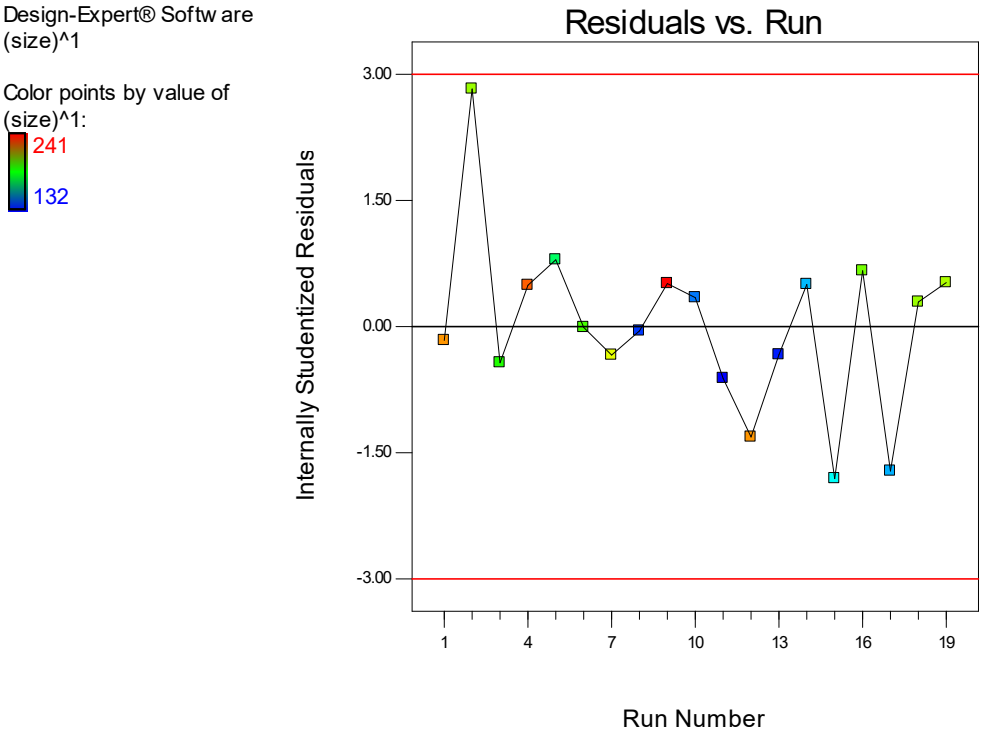

Figure 5. 6 Residual vs. run order plot for particle size

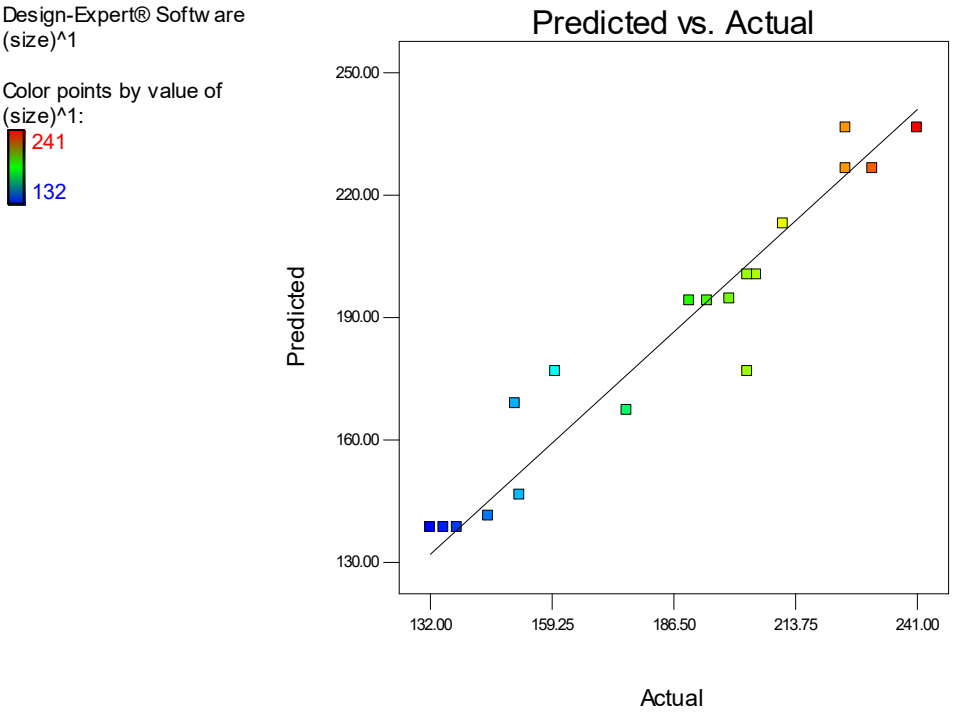

Figure 5. 7 Predicted vs. actual plot for particle size

Figure 5.4 is for the normal probability plot (normal plot of residuals) which shows whether the residuals follows a normal distribution or not and helps identify any specific patterns in the residuals indicative of requirement of transformations i.e. “S-shaped” curve, etc. normal plot for the current data show that data follows a straight line inferring the normal distribution of the residuals.

Residuals vs. predicted response (ascending values) plot tests if variance is distributed over the design constantly i.e. variance is not associated with the factor values as megaphone patterns (pattern like sign > or <) which indicate either decreasing or increasing residuals with increasing the factor values. This is a plot of the residuals versus the ascending predicted response values shown in figure 5.5.

As shown in figure 5.6, Residual vs. run order plots the residuals against the experimental run order i.e. order in which the experiments have been carried out. The plot with a random scatter of residuals indicate there is no time dependent changes in the residuals, i.e. there is absence of any time dependent variable among the variables selected or among the variables which has been not included in the DoE. If there is such Random scattered plot of residuals in the current analysis indicate no association of residuals with time and absence of any time dependent variable.

Predicted vs. actual plot shows correlation between the observed response values and actual response values. A good correlation between the predicted and actual values (data following a straight 45° line) shows that the model chosen for analyses of data is appropriate in predicting the responses all over the design matrix. Also, this plot helps to detect a value/ values that are not easily predicted by the model. As it can be seen from the figure, plot follows a 45° straight line indicating a close estimate of predicted values with actual values.

Plot of residuals vs. any factor evaluated if any association is there between the variance associated with different levels of factor i.e. any specific trends (+ve or –ve curvatures) associated with increasing level of each factor. As it can be seen from the figure 5.8, plots for each factor shows a random scatter over the increasing levels of factors indicating that the model is effective in accounting for the variance for each factor.

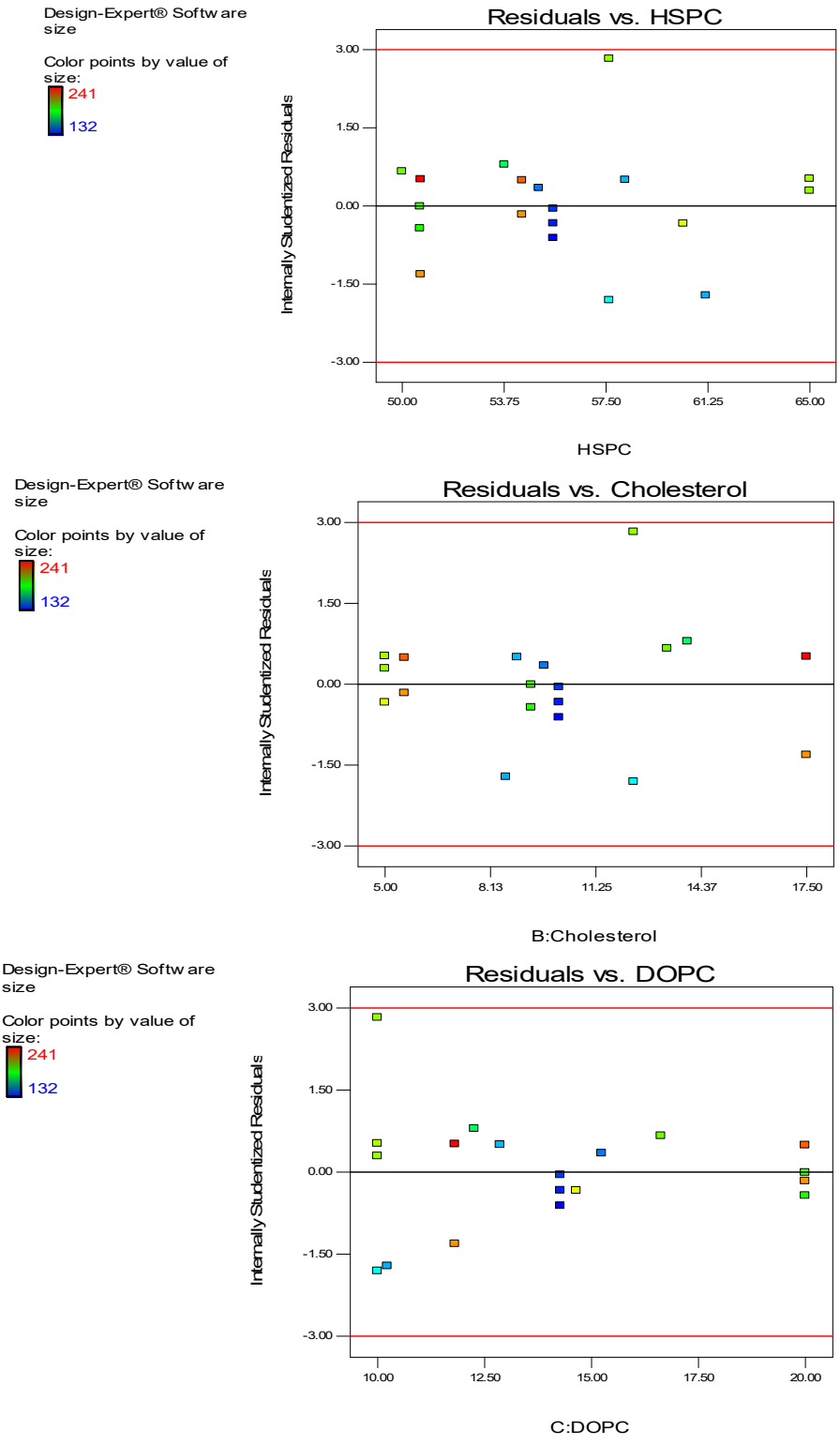

Figure 5. 8 Plots of residual vs individual factor to determine the time dependency of variable

Box-Cox plot of Ln (residuals sum of squares) vs. λ for power transformation helps select any power transformation of observed response values required for fitting the model based on the best λ value and 95% confidence interval around it. Plot in figure 5.9 shows the λ value of 1, which lies near the best λ value and within 95% confidence interval of it, indicating no requirement for any power transformation.

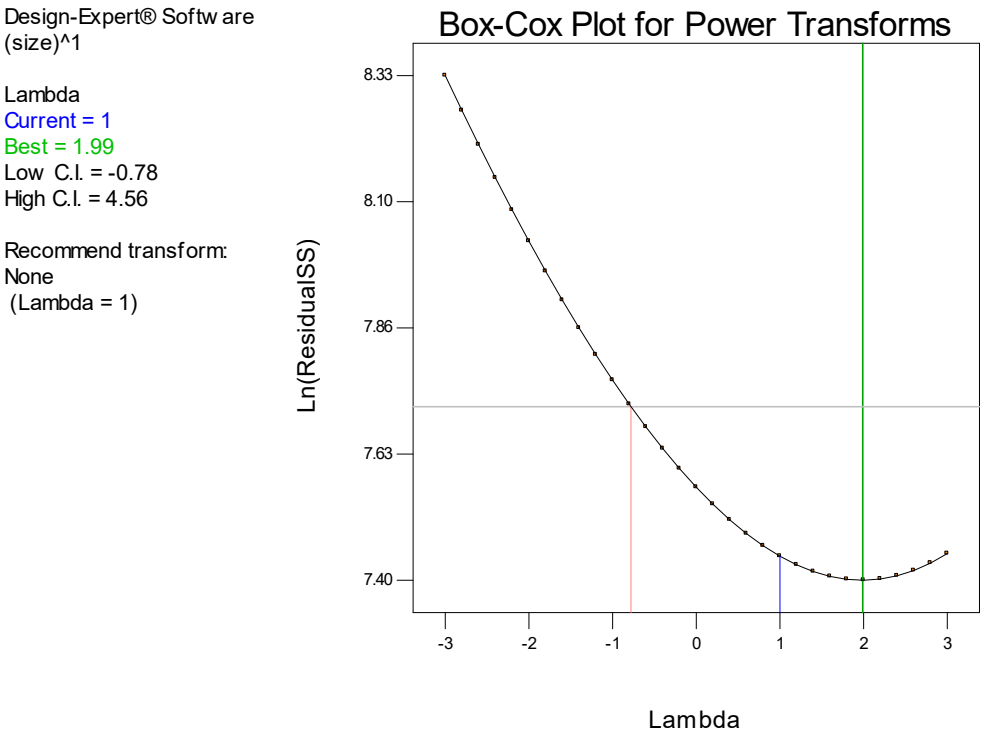

Figure 5. 9 Box-cox plot for particle size

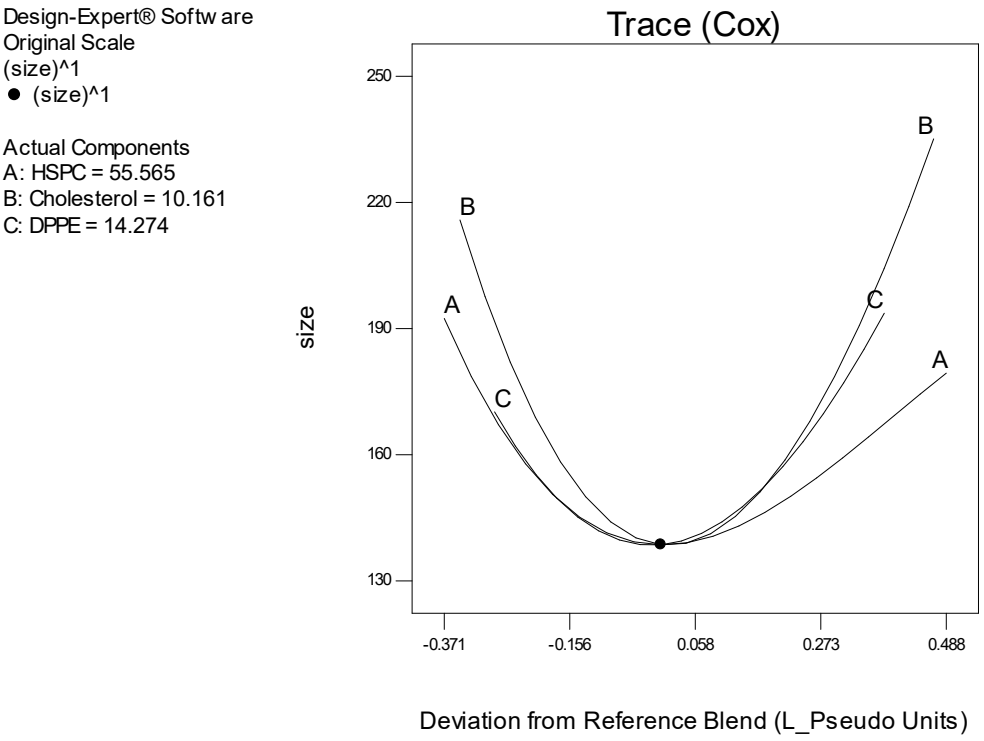

Figure 5. 10 Trace plot for particle size

Piepel's plot is a trace plot showing the effect of individual factors plotting the pseudo limits of one component keeping the ratio of the changeable amounts of each component kept constant against the response. The responses are plotted as deviations from the reference blend i.e. centroid (pseudo center point of the constrained design). As depicted in figure 5.10, Cholesterol has maximum effect on size of liposomes in comparison to other two variables.

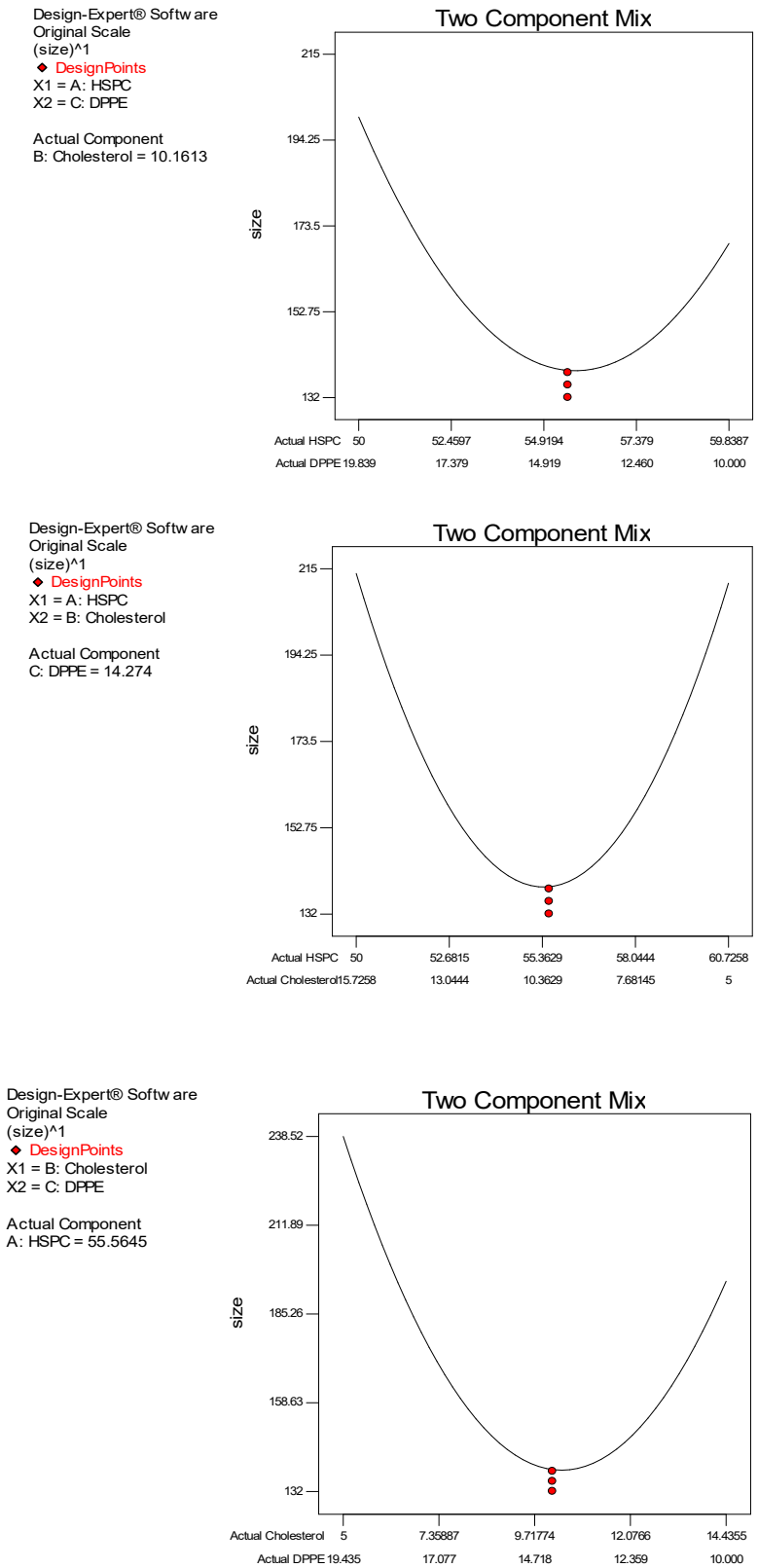

Figure 5. 11 Two component mixture plots for particle size

As depicted in figure 5.11, two component mix plots show the combined effects of two components on the response keeping the value of another component kept constant at its centroid value. As the ratio of HSPC:DPPE increases up to a point, with invariable mole % of cholesterol, particle size diminishes; after that point increase in ratio of HSPC:DPPE increases, particle size also increased. The size deviations, in turn, is explained by the relative small area per lipid adopted by PE lipids versus the PC lipids (33). Additionally, the inner monolayer favours inverted-cone shaped lipids, the fraction of DPPE is enhanced in the inner monolayer as DPPE possesses inverted-cone shape, leading to a more symmetric overall lipid distribution at lower HSPC:DPPE ratio, overcompensating for the size effect of HSPC (34). PC lipids tend to arrange themselves in very tight packing arrangement, so increase in mole % of HSPC helps in reducing size of vesicles. But after a certain point, it also appears that the PC lipids tend to shift a little more toward the bilayer interfaces, whereas the PE lipids found more of the interior space. This effect arising from the larger tendency of PC lipids to be hydrated in comparison to the PE lipids which form intra-lipid hydrogen bonds more easily thus at higher HSPC level, more lipid tends to be at outer interface leading to size increment with increase in HSPC level. At higher HSPC:DPPE ratio, this phenomena shows prominent effect on size leading to increase in liposomal size (35).

Cholesterol doesn't form a bilayer itself but it gets dissolved in the phospholipid bilayer (36). After a point, at higher concentration of cholesterol, irrespective of mole % of another component, more cholesterol molecules will be distributed in the phospholipid bilayer, causing an increase in the liposome mean diameter. At higher mole % of cholesterol incorporation into phospholipid bilayers, the small hydrophilic 3ß-hydroxyl head group of cholesterol is located in the vicinity of the lipid ester carbonyl groups, and the hydrophobic steroid ring orients itself parallel to the acyl chains of the lipid Thus, the movement of the acyl chains of the phospholipid bilayer has been restricted becoming the reason for failure of tight packing arrangement of other lipid components. It has been reported that higher cholesterol concentrations interfere with the close packing of the phospholipid bilayer by contributing to an increase in membrane fluidity which results in an increased distribution of aqueous phase within the liposomal vesicles. This explains the direct increase of liposomes mean diameter observed with higher cholesterol:HSPC ratio. Then as cholesterol:HSPC ratio decreases, size of the vesicles also decreases because of increasing mole % of HSPC resulting in tight packing of vesicles, up to a certain point. After that point, as mole % of HSPC increases, irrespective of mole % of cholesterol, HSPC tend to aligned

themselves at outer surface of vesicles that ultimately, increases the size of the liposomal vesicles. The same reasons are responsible for the size effects of DPPE:Cholesterol mole ratio on liposomes at invariable mole % of HSPC.

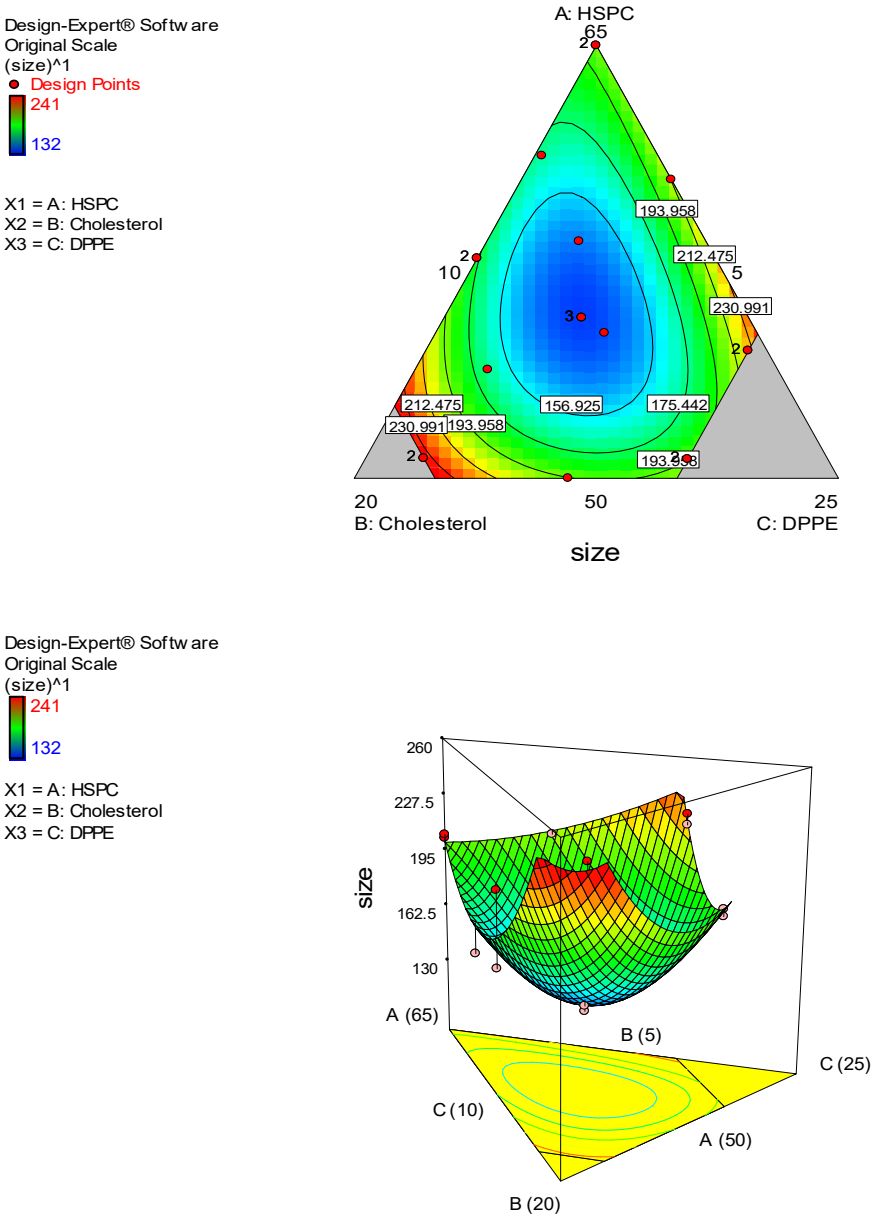

Figure 5. 12 Contour and response surface plot for particle size

Contour plot and response surface plot in figure 5.12 show effects of all three components on the particle size. To summarize, with increasing mole% of individual component brings about increment in size of liposomes up to a point after which increasing mole %, shows diminished liposome size. The effects can be explained with similar justifications mentioned under the two component mix plots also.

5.7.3 Statistical Analysis of Response 2 (Polydispersity Index-PDI)

Summary of the ANOVA results for different models as shown in table 5.12 depicts sequential p-values and Lack of Fit p-values along with Adjusted and Predicted R-squared values for different models.

Table 5. 12 ANOVA results summary for PDI

Source	Sum of Squares	df	Mean Square	F Value	p-value Prob > F	
Linear	0.41667	9	0.0463	4.04115	0.0395	
Quadratic	0.12716	6	0.02119	1.84996	0.2197	**Suggested**
Special Cubic	0.0793	5	0.01586	1.38433	0.3350	
Cubic	0.05487	2	0.02744	2.39476	0.1613	
Pure Error	0.08019	7	0.01146			

Source	Std. Dev.	R-Squared	Adjusted R-Squared	Predicted R-Squared	PRESS	
Linear	0.17622	0.58183	0.52956	0.40329	0.70901	
Quadratic	0.1263	0.82549	0.75837	0.59565	0.48045	**Suggested**
Special Cubic	0.11529	0.86577	0.79866	0.67005	0.39205	
Cubic	0.1225	0.88633	0.77266	-1.2423	2.66428	

Highest polynomial displaying highest Lack of Fit p-value 0.4815 i.e.> 0.1, was considered for model selection. Based on the criteria shown in table 5.13, special quadratic model was found to be best fitted to the observed responses. Cubic and other models were not suitable for prediction either due to low R-squared values and/or due to higher p value as contrasted to quadratic model.

Table 5. 13 ANOVA results for quadratic model

Source	Sum of Squares	df	Mean Square	F Value	p-value Prob > F	
Model	0.12191	6	0.02032	22.0169	< 0.0001	**significant**
Linear Mixture	0.0043	2	0.00215	2.32767	0.1399	
AB	0.0231	1	0.0231	25.0349	0.0003	
AC	0.00046	1	0.00046	0.49688	0.4943	
BC	0.00931	1	0.00931	10.0866	0.0080	
ABC	0.01022	1	0.01022	11.075	0.0060	
Residual	0.01107	12	0.00092			
Lack of Fit	0.00498	5	0.001	1.14581	0.4188	**not significant**
Pure Error	0.00609	7	0.00087			
Cor Total	0.13299	18				

As per table 5.14, the Model F-value of 22.0169 implies the model is significant. There is only a 0.01 % chance that a "Model F-Value" this large could occur due to noise. Values of "Prob > F" less than 0.0500 indicate model terms are significant. In this case AB, ABC are significant model terms. Values greater than 0.1000 indicate the model terms are not significant. If there are many insignificant model terms (not counting those required to support hierarchy), model reduction may improve model. The "Lack of Fit F-value" of 1.85 implies the Lack of Fit is not significant relative to the pure error. There is a 21.97 % chance that a "Lack of Fit F-value" this large could occur due to noise.

Table 5. 14 Summary of ANOVA result for special cubic model

Std. Dev.	0.1263	**R-Squared**	0.82549
Mean	0.45074	**Adj R-Squared**	0.75837
C.V. %	28.0198	**Pred R-Squared**	0.59565
PRESS	0.48045	**Adeq Precision**	9.84443

The "Pred R-Squared" of 0.5957 is in reasonable agreement with the "Adj R-Squared" of 0.7584 i.e. < 0.2. "Adeq Precision" measures the signal to noise ratio. A ratio greater than 4 is desirable. Ratio of 9.844 indicates an adequate signal. This model can be used to navigate the design space.

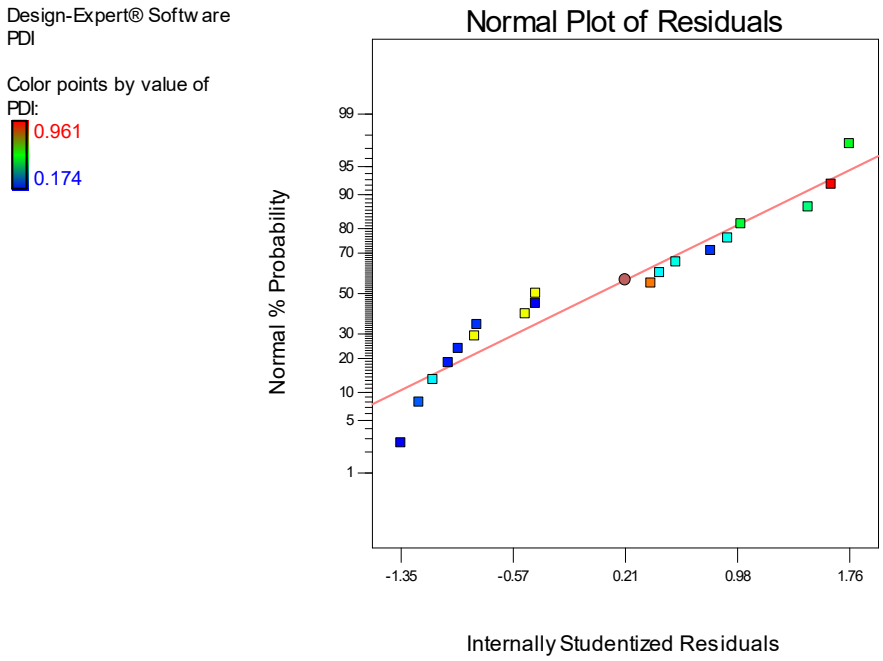

Figure 5. 13 Normal plot of residuals for PDI

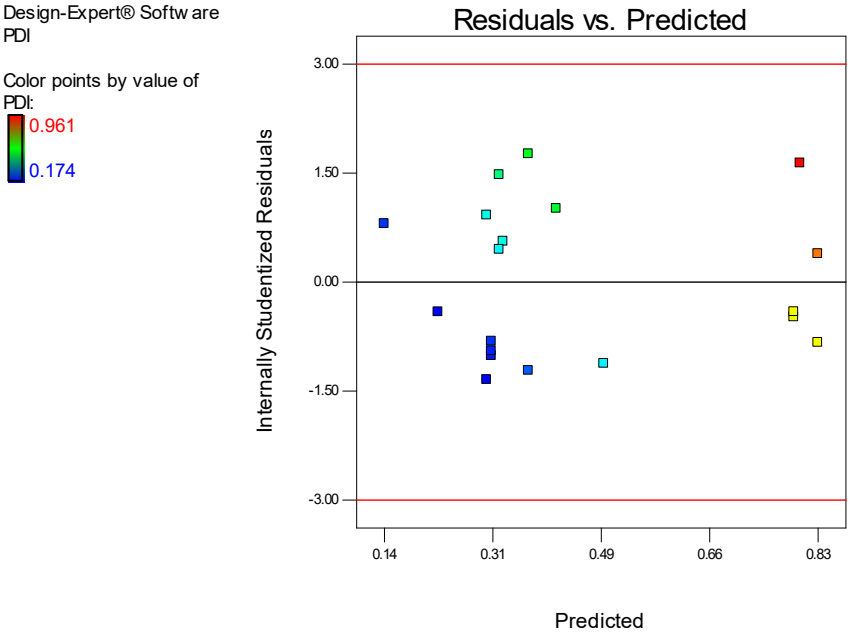

Figure 5. 14 Residual vs predicted pot for PDI

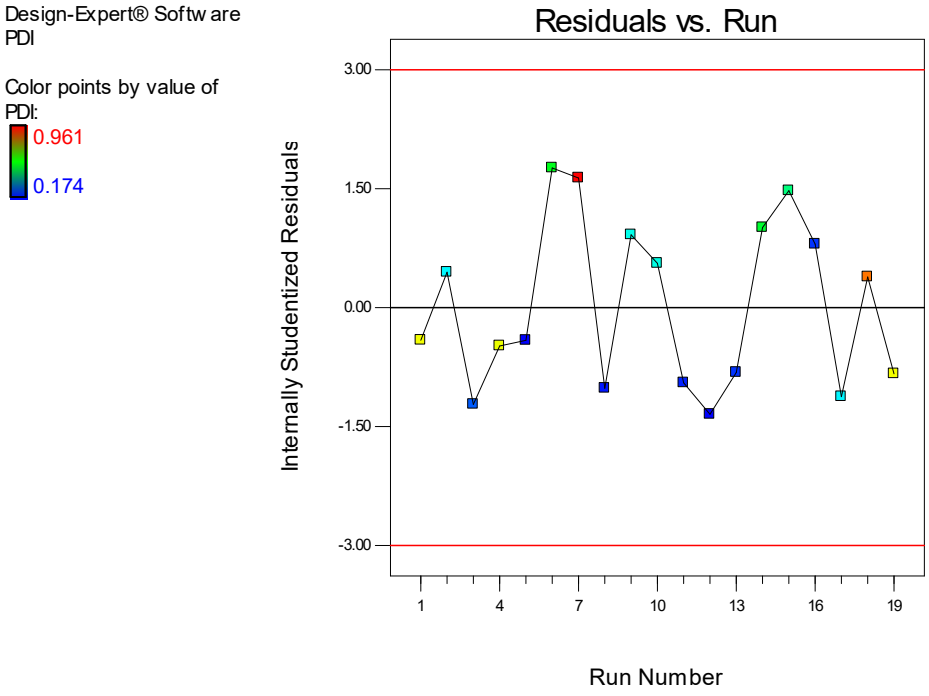

Figure 5. 15 Residual vs. run order plots for PDI

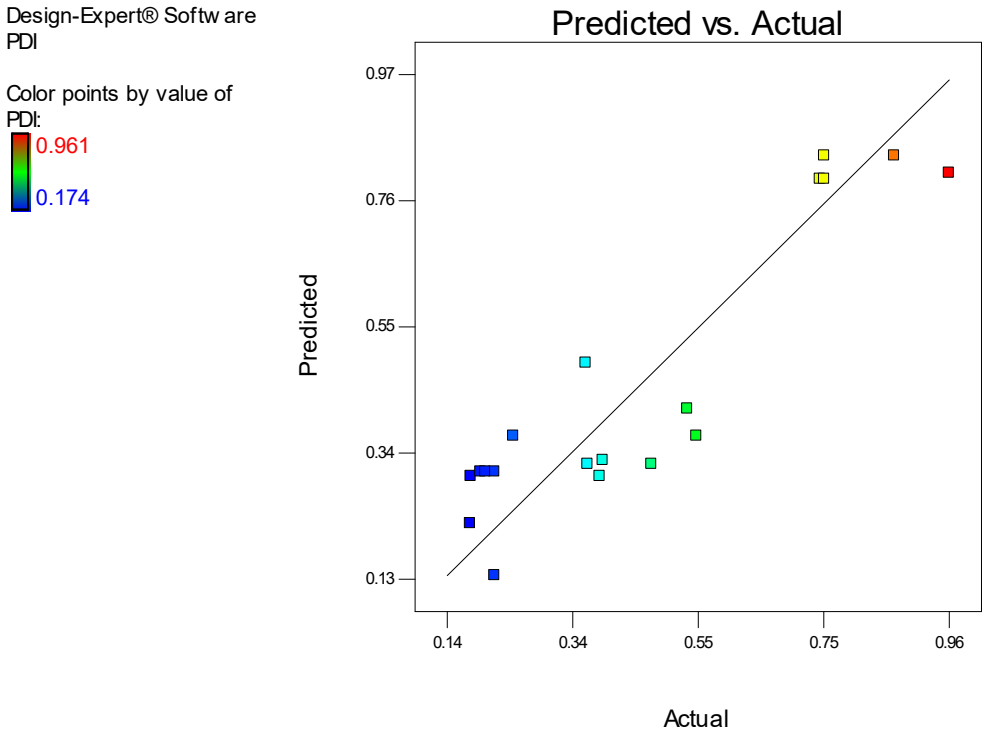

Figure 5. 16 Predicted vs. actual plot for PDI

Figure 5.13 is for the normal probability plot (normal plot of residuals) which shows whether the residuals follows a normal distribution or not and helps identify any specific patterns in the residuals indicative of requirement of transformations i.e. “S-shaped” curve, etc. normal plot for the current data show that data follows a straight line inferring the normal distribution of the residuals.

Residuals vs. predicted response (ascending values) plot tests if variance is distributed over the design constantly i.e. variance is not associated with the factor values as megaphone patterns (pattern like sign > or <) which indicate either decreasing or increasing residuals with increasing the factor values. This is a plot of the residuals versus the ascending predicted response values which is represented in figure 5.14.

As shown in figure 5.15, Residual vs. run order plots the residuals against the experimental run order i.e. order in which the experiments have been carried out. The plot with a random scatter of residuals indicate there is no time dependent changes in the residuals, i.e. there is absence of any time dependent variable among the variables selected or among the variables which has been not included in the DoE. If there is such Random scattered plot of residuals in the current analysis indicate no association of residuals with time and absence of any time dependent variable.

Predicted vs. actual plot shows correlation between the observed response values and actual response values. A good correlation between the predicted and actual values (data following a straight 45° line) shows that the model chosen for analyses of data is appropriate in predicting the responses all over the design matrix. Also, this plot helps to detect a value/ values that are not easily predicted by the model. As it can be seen from the figure 5.16, plot follows a 45° straight line indicating a close estimate of predicted values with actual values.

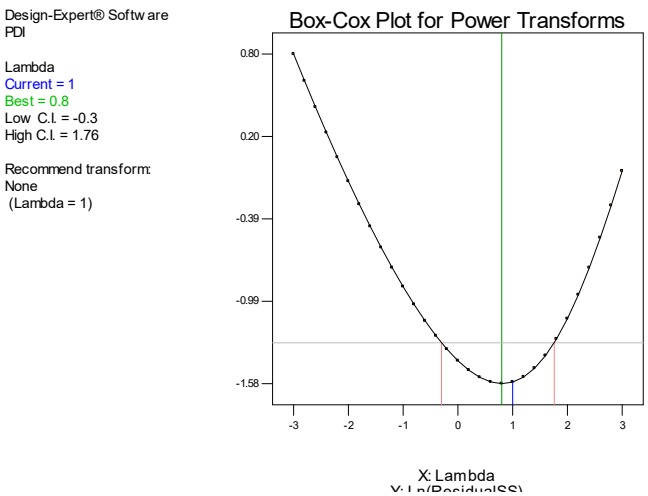

Figure 5. 17 Box-cox plot for PDI

Box-Cox plot of Ln (residuals sum of squares) vs. λ for power transformation helps select any power transformation of observed response values required for fitting the model based on the best λ value and 95% confidence interval around it. Plot in figure 5.17 shows the λ value of 1, which lies near the best λ value and within 95% confidence interval of it, indicating no requirement for any power transformation.

Piepel's plot is a trace plot showing the effect of individual factors plotting the pseudo limits of one component keeping the ratio of the changeable amounts of each component kept constant against the response which is shown in figure 5.18. The responses are plotted as deviations from the reference blend i.e. centroid (pseudo center point of the constrained design). HSPC and cholesterol, have the more impact on PDI than that of DPPE; give wide range of PDI with change in mole %.of HSPC or cholesterol.

.

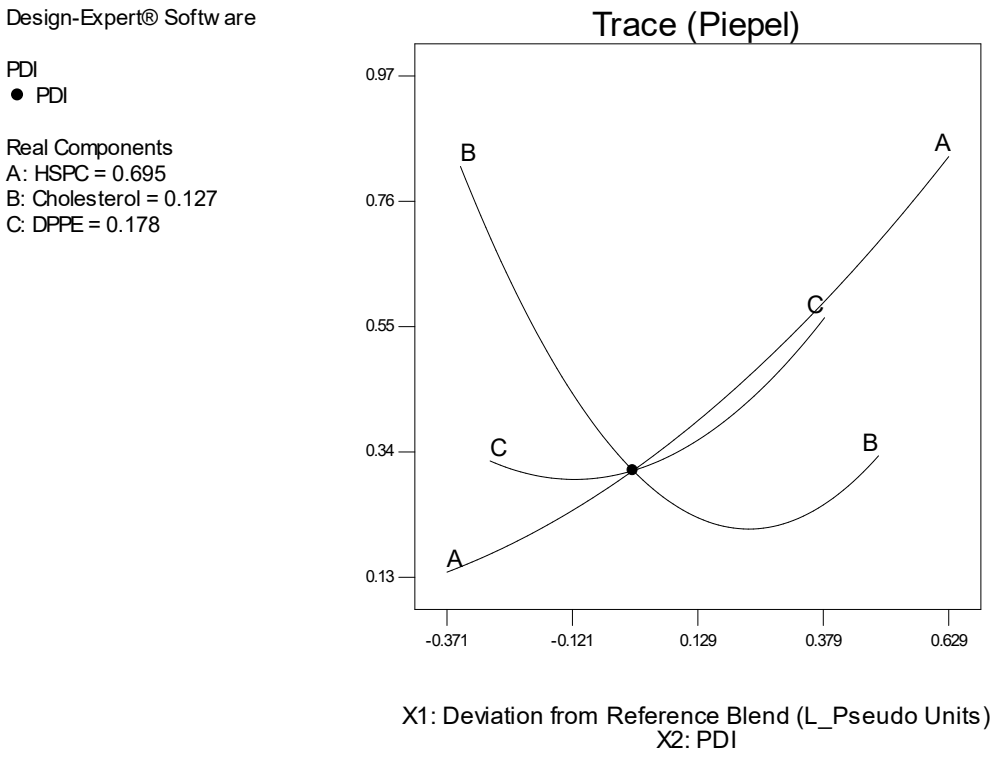

Figure 5. 18 Trace plot for PDI

As per two component mix plots graph in figure 5.19, they show the combined effects of two components on the response keeping the value of another component constant at its centroid value. As the ratio of Cholesterol:HSPC and Cholesterol:DPPE increases i.e. by increasing the mole % of cholesterol leads to lower PDI. The obtained results could also be explained based on the membrane rigidity resulted from CHO inclusion. It is well accepted that incorporation of CHO imparts rigidity to the bilayer membrane, thus improve the

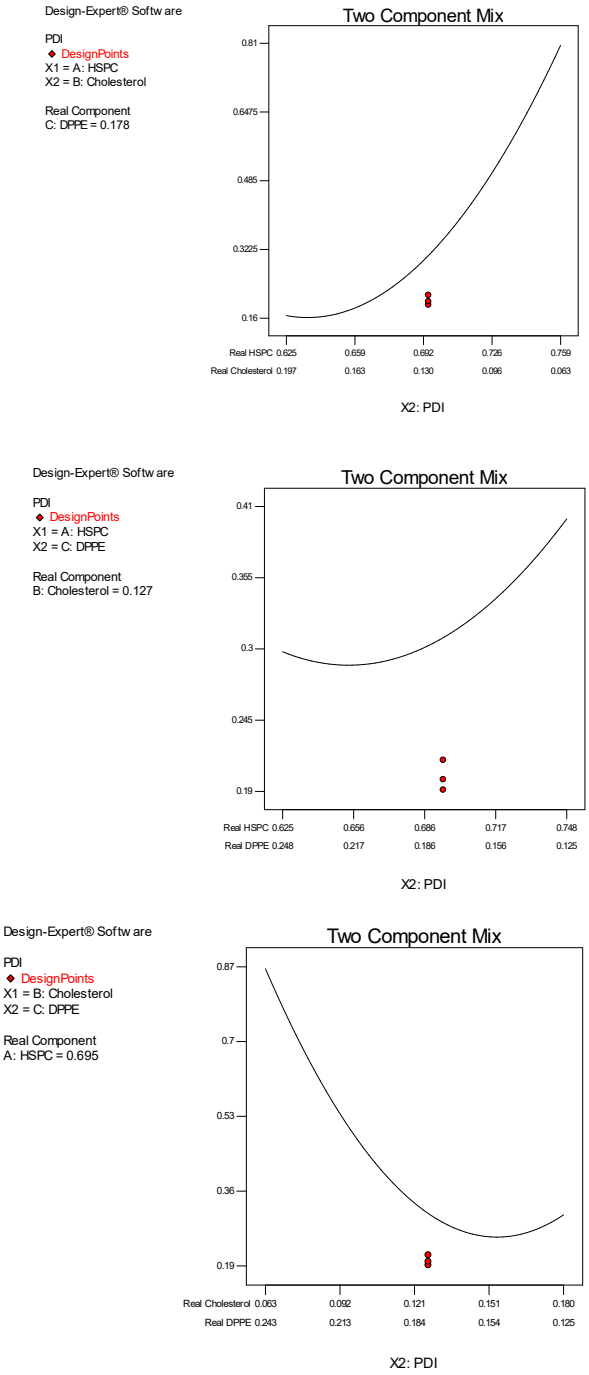

Figure 5. 19 Two component mixture plots for PDI

physical stability for liposomal system. Additionally, CHO can stabilize the bilayer

structure by eliminating the phase transition temperature peak of the vesicles, thereby strengthening the bilayer structures and diminishes bilayer micro fluidity. At low concentration of CHO, the vesicular membranes are more flexible and more liable to the effect of distortion. With increasing CHO concentration, the hardness of the membranes increased with increased resistance to alteration in size, thus producing vesicles with uniform size distribution.

Contour plot and response surface plot in figure 5.20 show effects of all three components on the particle size distribution. To summarize, increasing mole % of cholesterol resulting in improving particle size distribution while decreasing mole % of HSPC and DPPE resulting in higher PDI i.e. ununiform particle size distribution which was more prominent for HSPC mole % than DPPE.

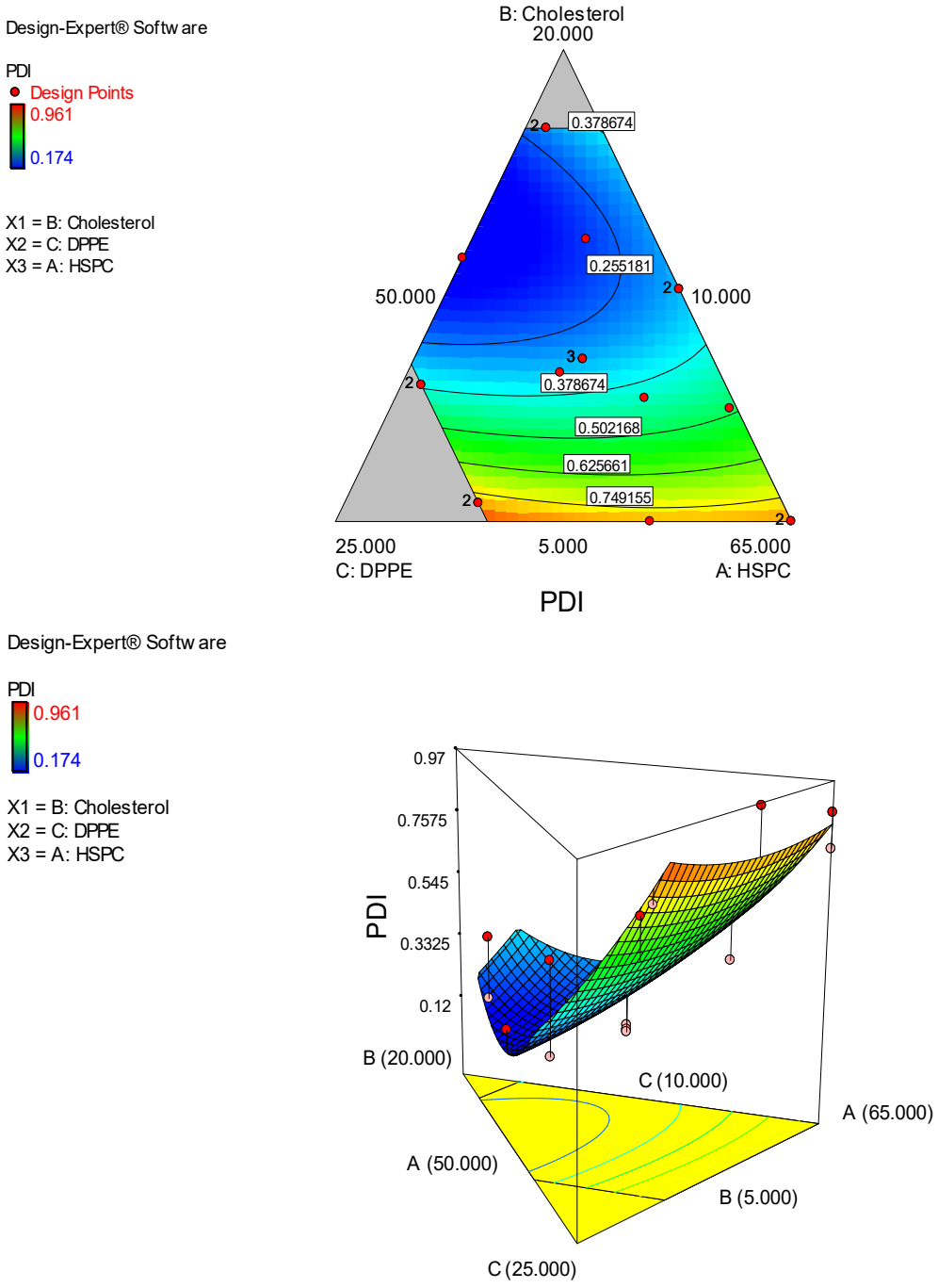

Figure 5. 20 Contour and response surface plot for PDI

5.7.4 Selection of Formulation Parameters

Constraints applied to select the best formulation parameters based on the desired particle size and polydispersity index is shown in table 5.15.

Table 5. 15 Constraints applied for selection of optimised batch

Name	Goal	Lower Limit	Upper Limit
HSPC	is in range	50	64.999
Cholesterol	is in range	5	17.5
DPPE	is in range	10	20
size	minimize	132	150
PDI	minimize	0.174	0.350

All the affecting factors were to be optimized within the range chosen for design matrix. Particle size was to be optimized at the minimum value possible in the range observed experimentally (130-150 nm) and PDI was to be optimized at the minimum value possible in the experimentally observed range of 0.174-0.350. Surface plots (Figure 5.21) demonstrate that the section with the lowermost particle size doesn't overlap with the section of lowermost PDI which entails a balance amid the certain parameters for assortment of an optimized batch. The optimization was grounded on the desirability criteria which makes the superlative trade off amid the constrains and choosing a group which gratifies the criteria, the best for optimization and weighs the prediction based on a desirability index which ranges from 0 (for the least suited combination) to 1 (the best suited combination). The desirability plot which represents the desirability index over the design is shown in figure 5.21 showing a flag where the optimized batch lies.

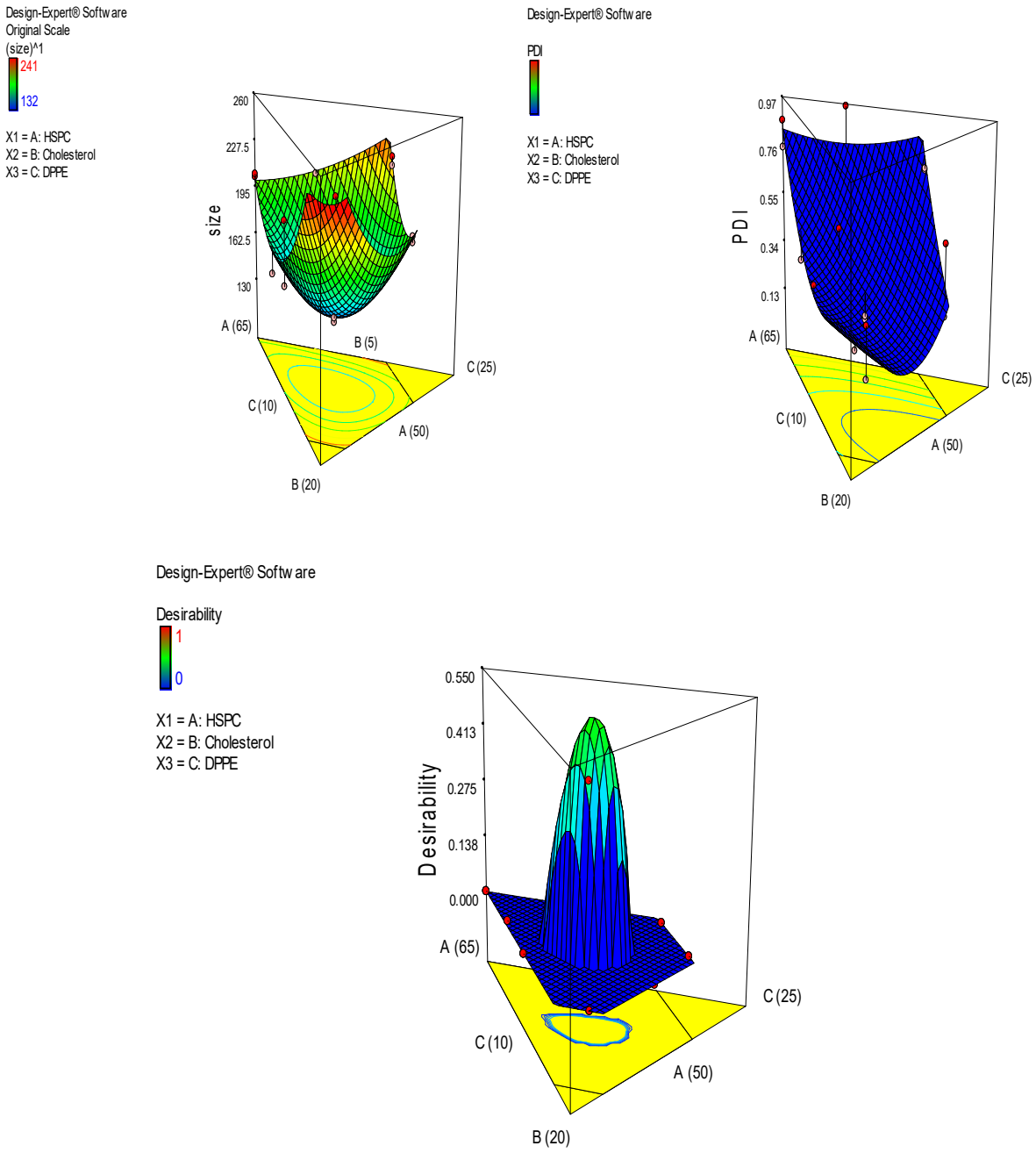

Figure 5. 21 Desirability plot for optimised batch selection

Based on the maximum desirability, one formulation (desirability 0.546) was found to best fit the selection constraints. Predicted responses of this batch were 140.73 nm particle size and 0.250 PDI shown in table 5.16.

Table 5. 16 Optimized batch parameters based on desirability criteria

HSPC (mole %)	Cholesterol (mole %)	DPPE (mole %)	Size (nm)	PDI	Desirability
54.605	11.246	14.15	140.473	0.251	0.54565

Additionally, selection criterial was also applied in order to select the design space within the design matrix where desired formulation responses can be observed. The selection criteria were particle size range of 100-125 nm and PDI of 0.150-0.200 and based on these criteria, following design space was found and shown in figure 5.22.

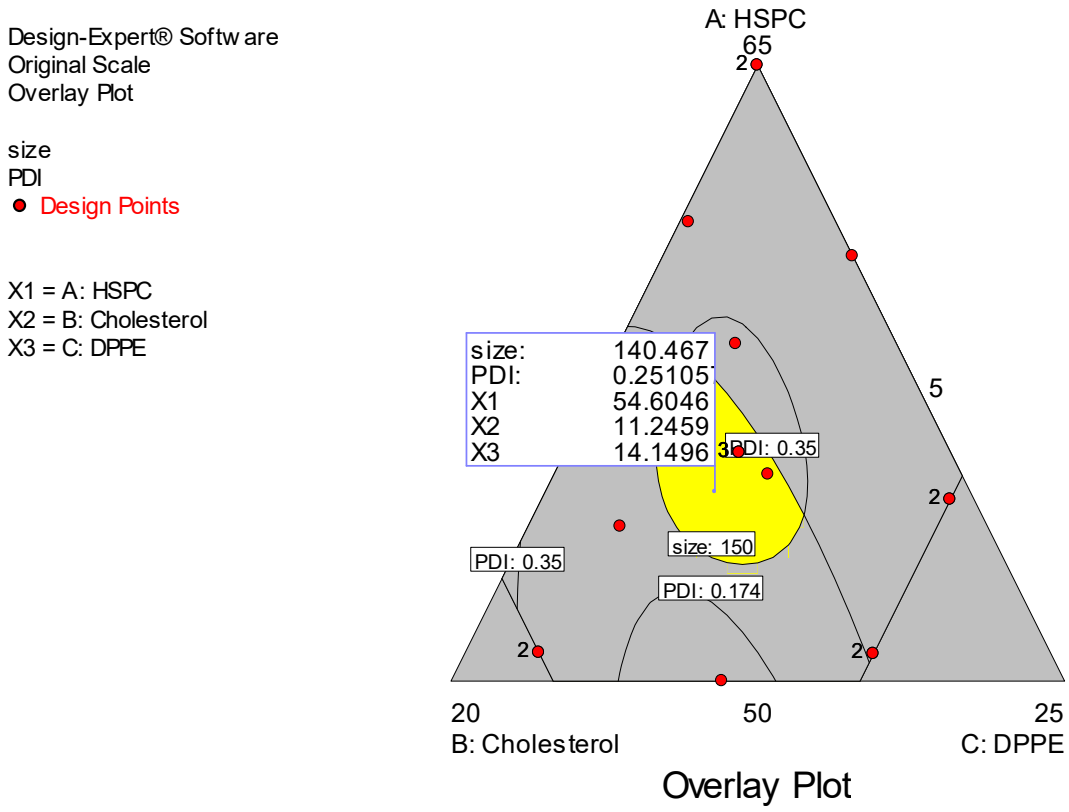

Figure 5. 22 Design space with optimum response parameters

5.7.5 Point Prediction and Confirmation

Table 5.17 below shows predicted response for the solution selected above along with the Standard deviation and 95 % confidence interval of the response. Confirmation of the response was done by carrying out the experiment using the selected factor values in triplicate.

Table 5.17 and figure 5.23 show and confirm that experimental and predicted values are in good agreement concluding the suitability of the selected model for optimization.

Table 5. 17 Size and PDI of predicted batches

Response	Predicted values		Experimental values					
			DOPE-A		DOPE-L		DOPE-H	
	mean	SD	Mean	SD	Mean	SD	Mean	SD
Particle size (nm)	140.473	3.48	131.6	2.25	136.1	4.3	141.3	6.2
PDI	0.251	0.059	0.265	0.044	0.225	0.038	0.225	0.035

Table 5.14 also shows and confirms that experimental and predicted values are in good agreement confirmed by calculating p values for both size and PDI. Results showed values of $p<0.05$, indicated no significant difference existed between practical value and standard value, concluding the suitability of the selected model for optimization.

DOPE-A

		Size (d.nm):	% Intensity:	St Dev (d.n...
Z-Average (d.nm): 131.5	Peak 1:	194.9	100.0	142.9
PdI: 0.265	Peak 2:	0.000	0.0	0.000
Intercept: 0.954	Peak 3:	0.000	0.0	0.000
Result quality : Good				

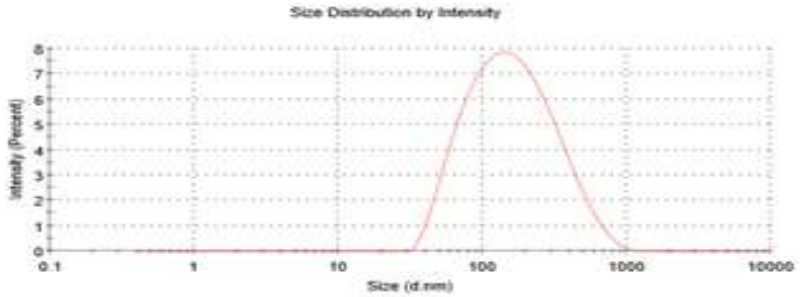

DOPE-L

		Size (d.nm):	% Intensity	Width (d.nm):
Z-Average (d.nm): 136.1	Peak 1:	157.7	100.0	62.73
PdI: 0.225	Peak 2:	0.000	0.0	0.000
Intercept: 0.945	Peak 3:	0.000	0.0	0.000
Result quality : Good				

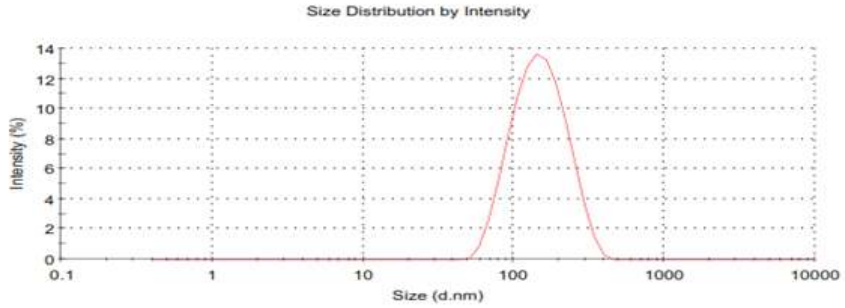

DOPE-H

		Size (d.nm):	% Intensity:	St Dev (d.n...
Z-Average (d.nm): 141.3	Peak 1:	174.9	100.0	88.26
PdI: 0.225	Peak 2:	0.000	0.0	0.000
Intercept: 0.959	Peak 3:	0.000	0.0	0.000
Result quality : Good				

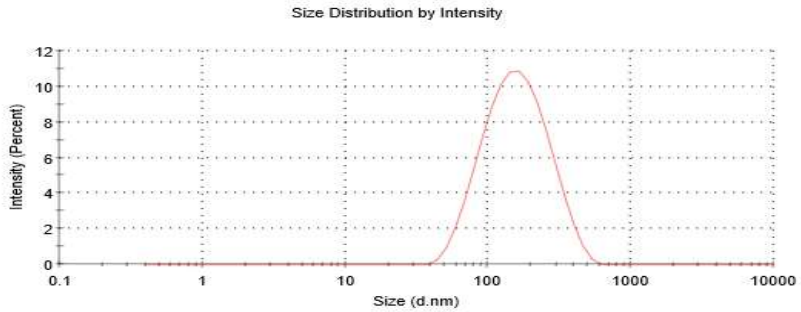

Figure 5. 23 Particle size distribution of liposomes for predicted batches formulated from modified lipids

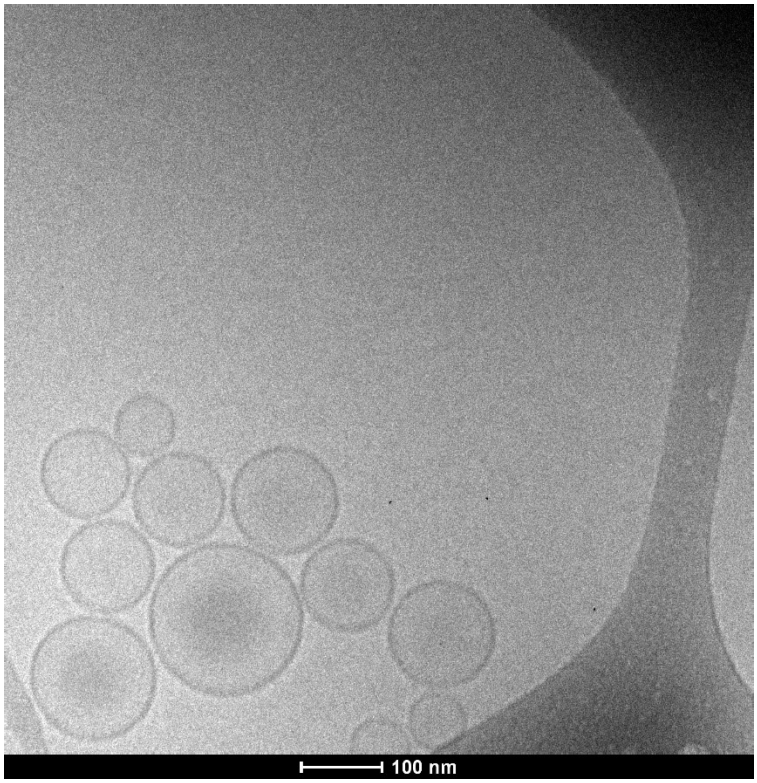

Figure 5. 24 Cryo-TEM image for lipoplex

Cryo-TEM image of optimised formulation also confirmed the size of liposome vesicle in the range of 100 to 150 nm with unilamellar structure.

5.7.6 Complexation efficiency and optimization of process parameters for complexation

The complexation efficiency of DOPE might be altered by introducing alkali amino acid residue to the primary amine of DOPE. For this reason, we examined the influence of the amino acids conjugated DOPE on the formation and complexation efficiency of lipoplex by using gel retardation assay. Complexation efficiency of formulations were further confirmed by Nanodrop UV spectroscopic determination. Charge dependent migration of cDNA towards anode under electric potential in gel retardation helps in evaluating the complexation efficiency of lipoplexes. In principle, when cDNA is complexed with cationic liposomes, migration of cDNA is retarded and cDNA remains inside the walls. However, if there is any uncomplexed cDNA, it will migrate on the gel under electromotive force giving a band visible under UV light. Images captured using image lab software on UV gel illuminator have shown the optimised L/P ratios of different polymers to cDNA. The data for different ratios for all the synthesised lipids have been given in table 5.18. Moreover, change in the zeta potential values of formed cationic liposomes formed complex also

indirectly predicted the DNA complexation to liposomal vesicles. The original zeta potential values of cationic liposomes formulated from arginine based liposomes was 53 ± 2.5 mV, histidine based liposomes was 45.3 ± 3.6 mV and that of histidine based liposomes was found to be 41.6 ± 2.9 mV which was changed after complexation to cDNA which is depicted in table 5.18.

Table 5. 18 Complexation efficiencies of liposomes at optimised L/P ratio and zeta potential of formed lipoplex

Modified lipid	L/P ratio	Gel electrophoresis	UV spectrophotometry	Malvern zeta sizer
		Maximum complexation (%)		Zeta potential (mV)
DOPE-H lipoplex	8	98.72 ± 2.35	96.57 ± 1.62	32.3 ± 4.6
DOPE-L lipoplex	6	96.43 ± 2.87	94.32 ± 2.41	28.5 ± 3.9
DOPE-A lipoplex	4	99.51 ± 3.48	98.86 ± 1.64	25.1 ± 4.1

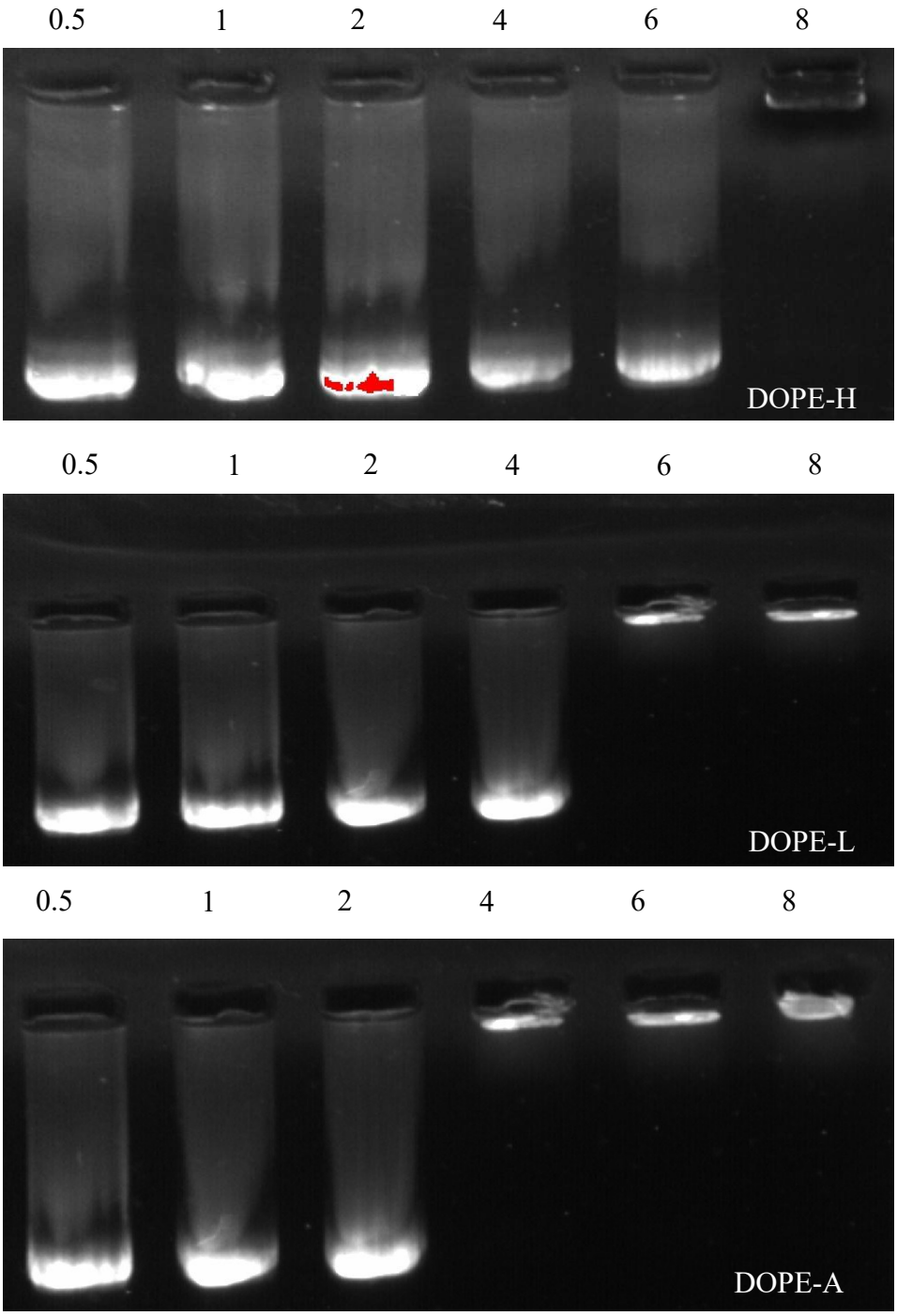

Figure 5. 25 Complexation efficiency of cationic liposomes formulated from modified lipids with p11 cDNA

The L/P ratio was different for lipoplex formulated from different synthesised lipids because all the conjugated amino acids have different conjugation efficiencies to DOPE. Moreover, all conjugated amino acids possess different charge at physiological pH 7.4. The proposed amino acids modifications of DOPE affect the ionizing property of modified DOPE lipid at DNA binding condition; therefore, different L/P ratio was required for the binding of DNA to formulated cationic liposomes to compensate for availability of different ionizable properties. Lipoplexes formulated from different amino acids showed a steady decrease in L/P ratio required for complete retardation of cDNA in trend of DOPE-H > DOPE-L > DOPE-A as shown in table 5.18 and figure 5.25. This also, means that to deliver same dose of cDNA, higher quantity of lipids in form of lipoplex, would be introduced in the body. The difference in L/P ratio suggesting increase in charge density after conjugation of alkaline amino acids to DOPE.

We have conjugated arginine, lysine and histidine to a natural phospholipid, phosphatidylethanolamine (PE), DOPE, by forming an amide linkage between the amino group of PE and carboxy group of arginine. Lipids have been provided with positive charge by introduction of the ammonium functions by lysine (pKa= 6.04), histidine (pKa=10.54) and guanidine group provided by arginine (pKa=12.48). Based on pKa values, we can conclude that at physiological pH, all modifications possess different positive charge density resulting in different L/P ratio for maximum complexation, arginine being highest and histidine lowest.

Optimization of process parameters

pH

Arginine, lysine and histidine have basic side chains at neutral pH. Their side chains contain nitrogen and resemble ammonia, which is a base. They tend to bind protons because of their high pKa values and transform itself into positive charged moiety. Their pKa values are high enough that they tend to bind protons. Consequently, pH plays an important part in protonation of amino acids and amino acid being an integral part in providing positive charge to DOPE which was then employed in formulation of liposome (37). These alkaline amino acids possess diverse positive charge density at acidic, basic and neutral pH values. Based on their pKa values; all amine groups of lysine, arginine and histidine modifications of DOPE hold (+1) charge at weakly acidic condition at pH 5, while at neutral pH only 25 % of amine groups present in histidine modification of DOPE possesses (+1) charge and at weakly basic condition i.e. at pH 9, only arginine amine group (around 50 %) hold its positive charge because of its high pKa value in comparison to lysine and histidine. Based

on this charge diversity, lipoplexes formulated from these amino acids modified DOPE showed different complexation efficiencies as depicted in figure 5.26.

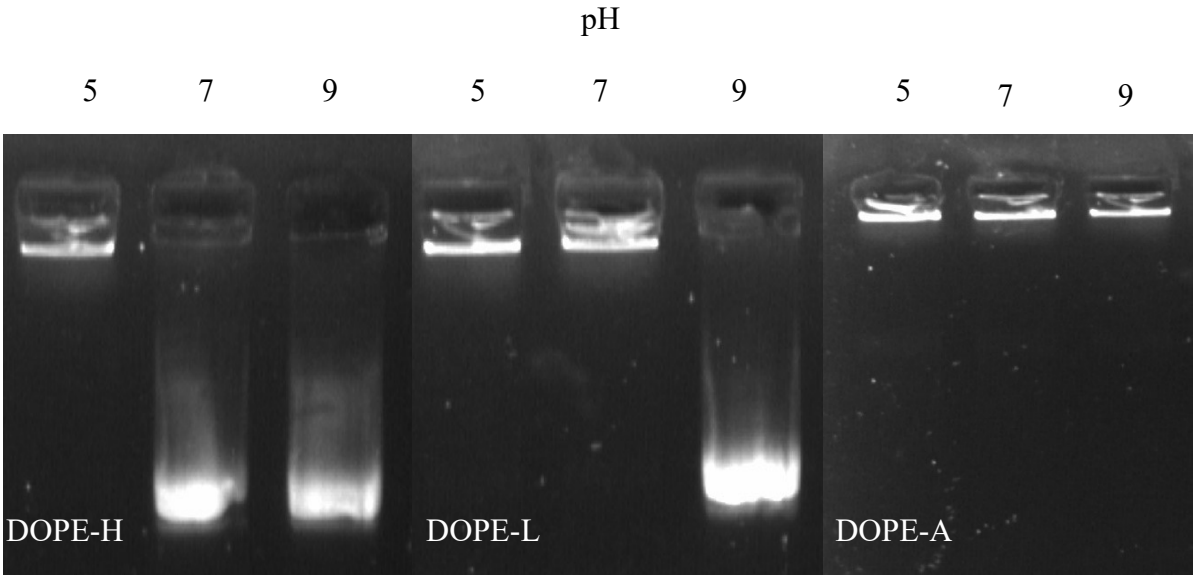

Figure 5. 26 Effects of pH on complexation efficiency lipoplex

Incubation temperature

In order to investigate the effect of temperature on complexation efficiency of lipoplexes incubated with cDNA at different temperatures i.e. at cold temperature 20° C ± 2° C, 37° C ± 2 °C temperature (RT) and 55 °C ± 2 °C temperature for 30 min of incubation period. It was observed that for a constant incubation period, temperature affected the complexation efficiency of liposome. For 30 minute incubation, the complexation efficiency at L/P ratio which gave maximum complexation, there was no change in complexation efficiency at 37° C and 55 °C for all the formulations but drastic change was found in complexation efficiency at 20° C temperature as shown in figure 5.27. None of the formulations, was able to be complexed with cDNA at this temperature could be due to the decreased mobility of cDNA molecules rendering the flexibility in the cDNA structure to approach the cationic surface. Also, decreasing temperature also decrease the movement of PEG chains extending on the surface of liposomes which allows closer approach of the cDNA nearer to the cationic charge bypassing the PEG chains (38).

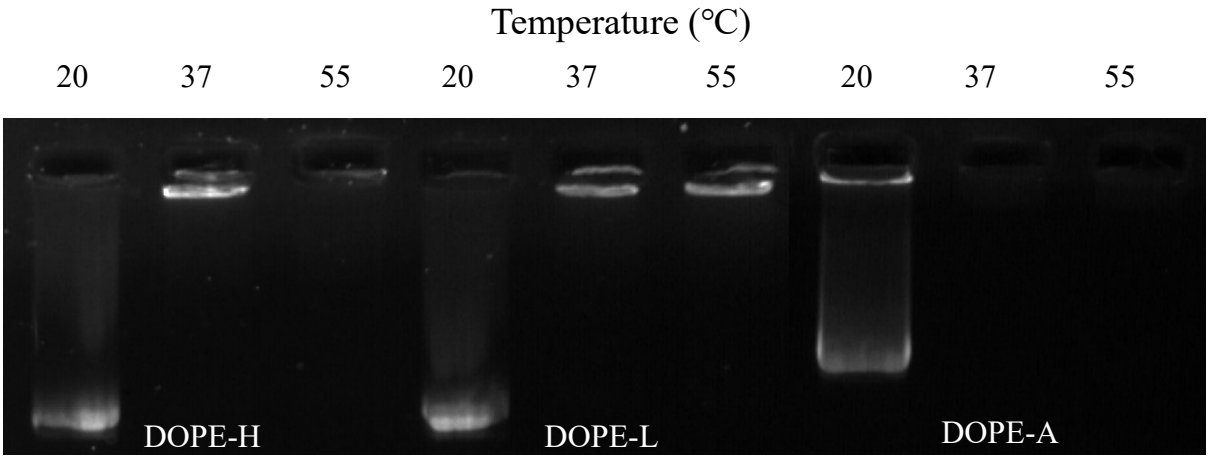

Figure 5. 27 Effect of temperature on complexation efficiency of lipoplex

5.7.7 Electrolyte induced flocculation study

Electro flocculating property of the liposomes was determined by measuring the absorbance at 400 nm and also the size of the liposomes and the results obtained were as shown in table 5.19 and graphs below in figure 5.28. After administration, liposomes would be exposed to various ions including sodium, calcium, potassium, chloride in blood which may affect the stability of liposomes (39). Because of flocculation, size of the liposome also increases, which results in increase in its macrophage uptake which ultimately lead to its clearance from the body. From this study it was found that all liposomal preparations, formulated from amino acid conjugated DOPE, was able to resist aggregation due to external electrolytic influence up to 3 % concentration of Na_2SO_4. At higher electrolyte concentration the steric barrier was lost, subsequently liposomal aggregation was found exceeding 3% Na_2SO_4 concentration. This was concluded by abrupt increase in the absorbance after 3% Na_2SO_4 concentration.

Table 5. 19 Effects of sodium sulphate concentration on modified liposomes

Concentration of Sodium Sulphate (%)	Absorbance			Size (nm)		
	DOPE-H	DOPE-L	DOPE-A	DOPE-H	DOPE-L	DOPE-A
0	0.399	0.364	0.253	112.27	109.62	107.38
0.5	0.412	0.391	0.251	127.61	117.94	112.30
1	0.401	0.395	0.276	126.72	119.37	124.52
2	0.429	0.412	0.293	159.41	147.17	132.61
3	1.044	0.927	0.907	454.17	413.08	393.72
4	1.103	0.984	0.931	467.12	451.65	412.73
5	1.091	0.993	0.948	444.51	462.74	431.82

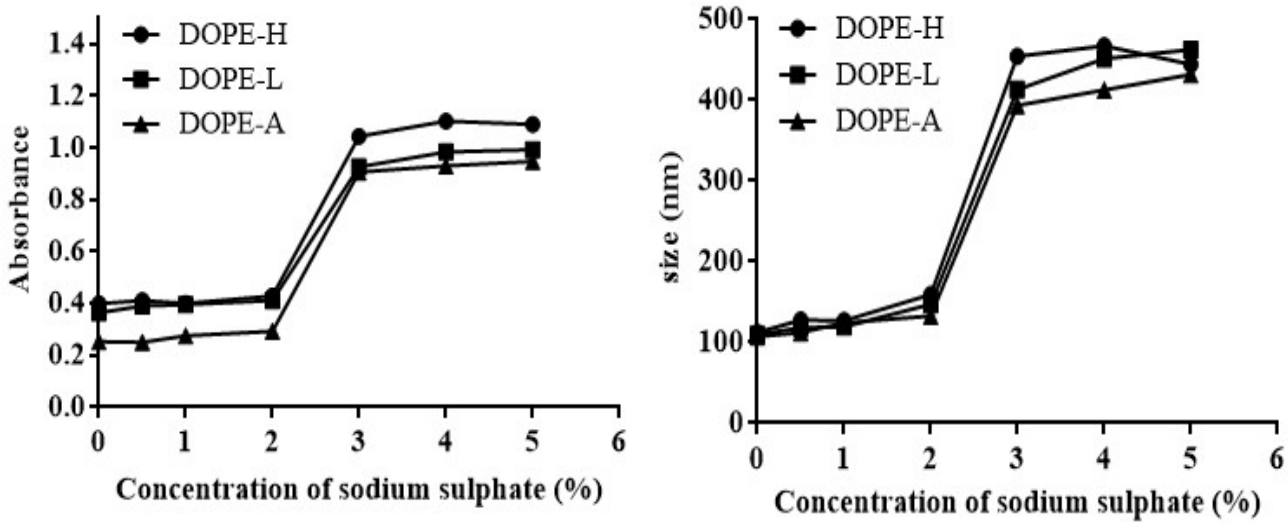

Figure 5. 28 Effects of sodium sulphate concentration on liposome formulated from modified lipids

5.7.8 Heparin polyanion competition assay

The resistance to heparin competition assay depends on ratio of DNA to heparin (40). Additionally, it also gives idea about if the formulations were made at appropriate L/P ratio as it directly extrapolates to their transfection efficiency. Stability up to heparin/DNA weight ratio of >1is considered appropriate for achieving adequate *in vivo* stability (41). All the lipoplex formulations were evaluated at their optimised L/P ratio. As shown in table 5.20 and figure 5.29, It was found that lipoplex consisting of DOPE-H was stable to heparin up to weight ratio of 1.0 (heparin: DNA) ; similar way, lipoplex consisting of DOPE-L was stable to heparin up to weight ratio of 2.0 and lipoplex of DOPE-A was stable up to weight ratio of 3.0. Hence, lipoplex formulated from DOPE-A was having higher resistance to

heparin displacement than lipoplex formed from the lipids DOPE-L and DOPE-H. This can be attributed to high charge density of arginine modified DOPE than DOPE modified by Lysine and Histidine.

Table 5. 20 effect of heparin concentration on complexation efficiency

Formulation	Heparin:cDNA (w:w)
DOPE-H	1:1
DOPE-L	1:2
DOPE-A	1:4

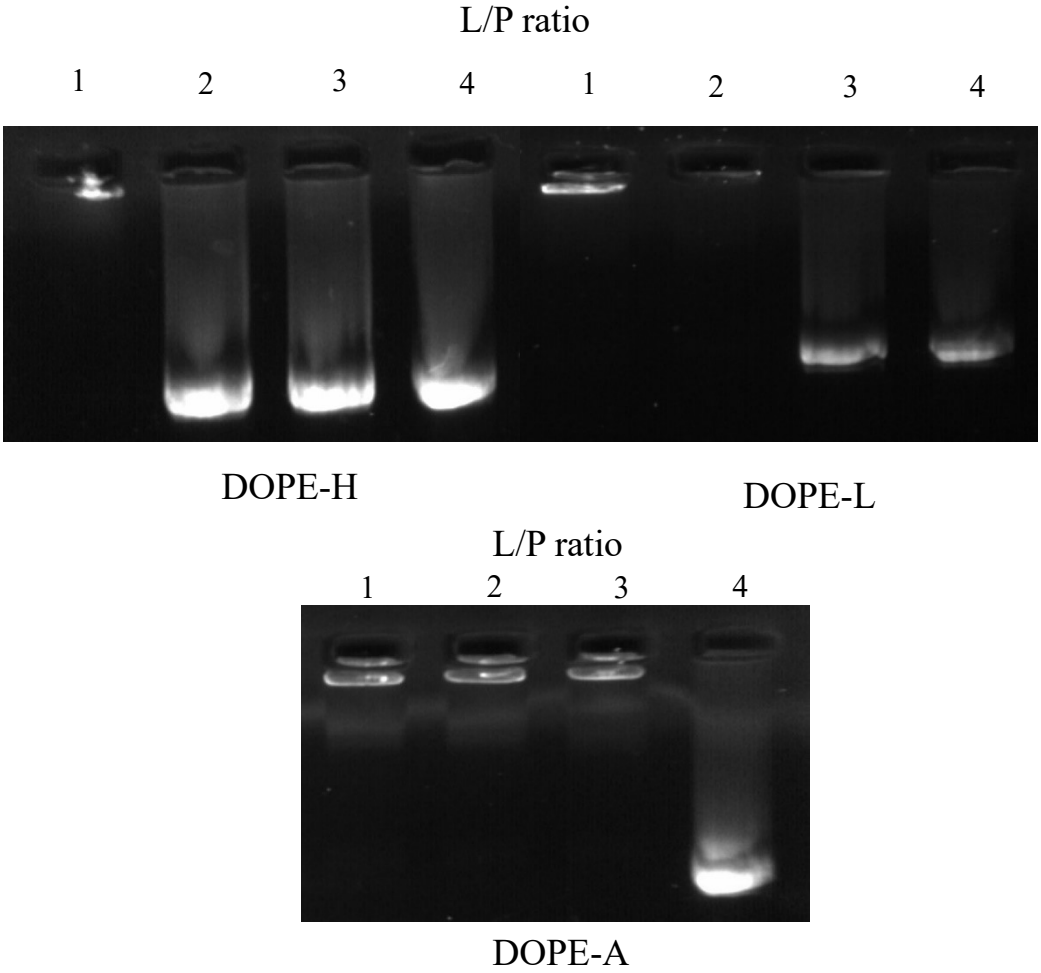

Figure 5. 29 Stability of lipoplex formulated from modified lipids in presence heparin

5.7.9 Serum stability study

Non-viral gene delivery vectors like lipoplex should have the property to protect cDNA from degradation/detachment by DNAses, especially those present in serum if administration is meant for intravenous route or in organs where negatively charged proteins can affect the stability of formulation (42). The ability of synthesised lipids to protect DNA in blood circulation can be evaluated by incubating lipoplex formulation with (50 % v/v) serum to simulate the cell culture media. The serum stability is essential since the polyanions present in the extracellular matrix *in vivo* and *in vitro* cell culture media can compete with cDNA and displace them, thereby exposing the degradable conditions. Table 5.21 and figure 5.30 showed the results of serum challenge study. All the formulations based on amino acids modified DOPE, showed good stability in serum challenge study in comparison to naked cDNA. They were evaluated at their optimised L/P ratio. The analysis of cDNA detachment from lipoplex formulations after incubating with serum showed that lipoplex formulated from arginine modified lipid exhibited maximum stability with minimum detachment of cDNA from lipoplex owing to its high charge density resulting in strong attachment of cDNA to positively charged liposome. Less charge density of Lysine and Histidine modified DOPE showed less stability with more amount of cDNA detached from lipoplex as time passes, showing their low affinity of complexation towards cDNA.

Table 5. 21 cDNA retention efficiency of lipoplex in presence of serum

	% cDNA retained			
Time (H)	**Naked cDNA**	**DOPE- H**	**DOPE- A**	**DOPE- L**
0	100	100	100	100
1	81.37 ± 2.68	98.12 ± 3.62	99.65 ± 0.61	99.51 ± 2.85
2	58.68 ± 3.89	96.39 ± 2.71	98.32 ± 1.70	98.35 ± 2.63
4	24.53 ± 4.08	91.71 ± 3.18	96.55 ± 1.67	94.66 ± 1.94
8	-	83.36 ± 2.69	95.36 ± 2.09	90.93 ± 3.48
16	-	81.25 ± 4.23	89.64 ± 4.27	86.64 ± 4.30
20	-	74.28 ± 4.92	87.85 ± 1.65	83.17 ± 2.62
24	-	69.64 ± 3.56	86.94 ± 3.46	82.94 ± 1.53

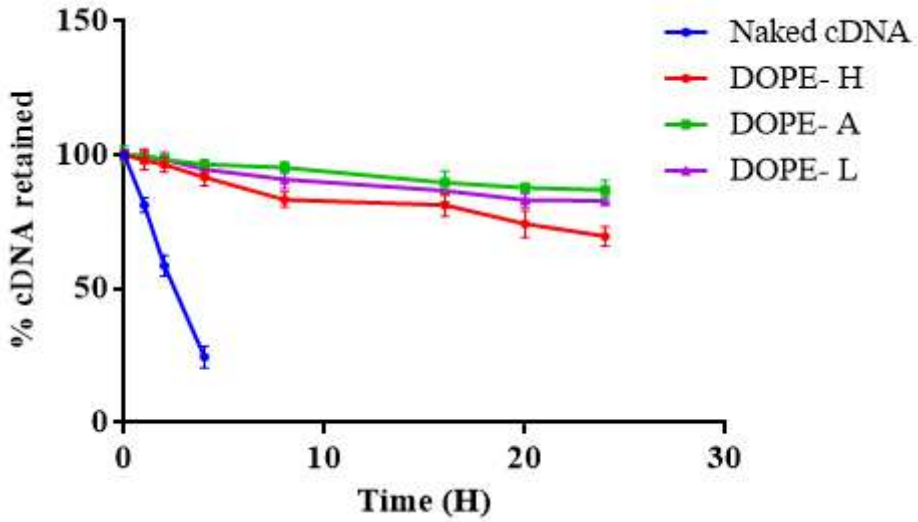

Figure 5. 30 Serum stability studies lipoplex formulated from modified lipids

5.7.10 Haemolysis study

When liposomes are developed as systems to deliver drugs to specific cell types after circulating for long time periods in the bloodstream, their compatibility with blood is of increased importance. Haemolysis studies should be performed during the development of such nano sized formulations. Though cationic charge is a facilitator of cell membrane attachment and subsequent endosomal uptake, however too much of cationic charge leads to membrane destabilization and haemolysis (43). During haemolysis, lipids produce nano-sized pores in cell membrane inducing an influx of solutes into the cells which causes rupture by destabilization of membrane and release of haemoglobin molecules (44). Along with charge, the lipid structure and confirmation also play important role in mediating toxicity, wherein rigid and helical confirmations are said to be more membrane permeabilizing. Herein, we studied haemolysis caused by different liposomal formulations at varied concentration ranges from 0.01 mM to 5 mM, formulated by synthesised lipids as cationic charge created by modifications of DOPE by alkaline amino acids may lead to increase in haemolytic potential of formulated lipoplexes with DOTAP as negative control and PBS as positive control. Results in table 5.22 and figure 5.31 showed that even at lipid concentration as high as 5 mM, all cationic liposomes showed haemolysis less than 5 % in comparison to lipoplex composed of DOTAP as cationic lipid which showed 81.72 % of haemolysis. Low haemolytic potential of prepared liposomes concludes their low toxicity to blood as well as normal cells.

Table 5. 22 Haemolytic potential of modified lipoplex

Concentration (mM)	% Haemolysis				
	DOPE-H	DOPE-L	DOPE-A	DOTAP	PBS
0.01	0.63	0.76	0.97	9.62	0.06
0.05	0.94	1.08	1.38	15.94	0.15
0.10	1.26	1.63	1.95	26.34	0.17
1	1.82	1.85	2.18	51.38	0.18
2.5	2.41	3.12	3.91	68.30	0.21
5	3.96	4.23	4.62	81.72	0.26

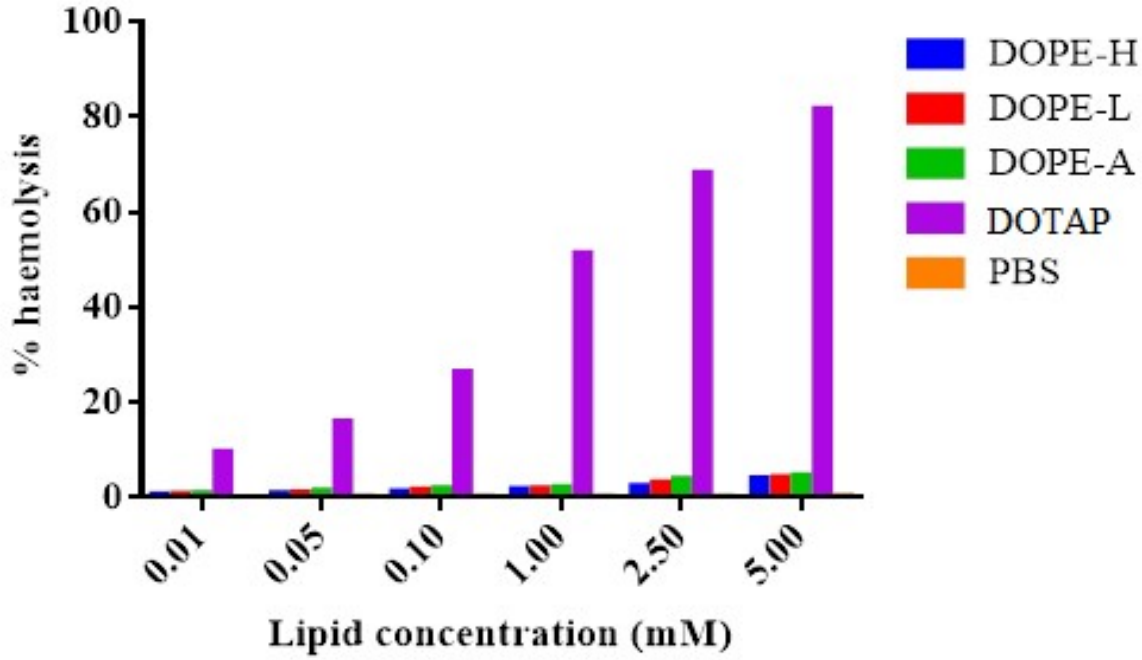

Figure 5. 31 Graph of haemolytic potential of lipoplex formulated from modified lipids

5.7.11 Erythrocyte aggregation study

During aggregation process, it is a property of cationic lipid molecules to interact with erythrocyte surface and then bridge/chains inter-tangle with each other leading to flocculation and aggregation. However, as observed in figure 5.32, lipoplex incorporated with synthesised lipids, showed no sign of aggregation renders the lipoplex formulation safe to be delivered by systemic route with comparison to lipoplex incorporated DOTAP lipid.

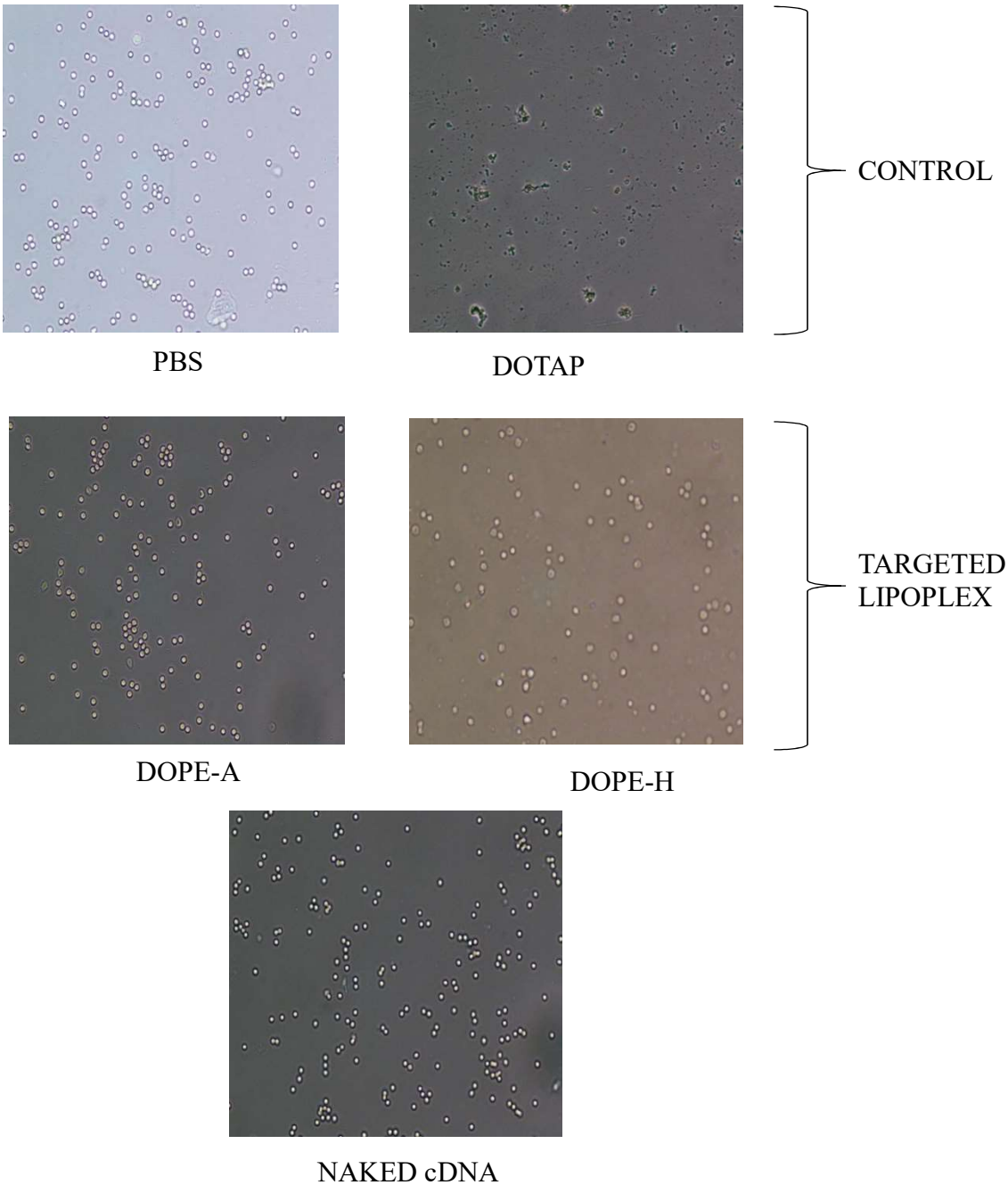

Figure 5. 32 Erythrocyte aggregation potential of lipoplex formulated from modified lipids

5.7.12 MTT assay

The cytotoxicity of the alkali amino acid based cationic liposomes was investigated in SHSY5Y cells as shown in figure and compared with that of Lipofectamine™ 2000. All the lipoplex formulations showed less cytotoxicity when they were compared to control Lipofectamine™ 2000. As shown in figure order of their cytotoxicity behaviour at same N/P ratio is:

Lipofectamine™ 2000 > DOPE-A > DOPE-L > DOPE-H

The existence of multivalent cationic lipid DOTAP in Lipofectamine™ 2000 was the prime reason of its maximum cytotoxicity among all the formulations containing cationic charged lipids modified with alkali amino acids. Lipoplex formulated from modified DOPE lipids also showed some sort of cytotoxicity because of the presence of DOPE itself. Moreover, it was stated that DOPE increases toxicity to various immune effector cells showing its cytotoxic character. The low cytotoxicity of amino acid based cationic liposomes can be attributed to the presence of ester bonds and amino acid analogues as well as rapid biodegradability post-transfection. Among all the synthesised lipids, arginine modified lipids showed somewhat more toxicity at given N/P ratios than that of leucine and histidine modified lipids because of its highest charge density at any given pH. But this more charge density of arginine based lipids resulting in less requirement of lipids for the maximum complexation of cDNA. DOPE-A required N/P ratio of 2 for maximum complexation while for the same complexation efficiency, the least cytotoxic lipid i.e. DOPE-H required N/P ratio of 4. Now at this ratio as shown in figure 5.33, DOPE-H showed more cytotoxic character than the lipids required for maximum complexation in case of DOPE-A lipid.

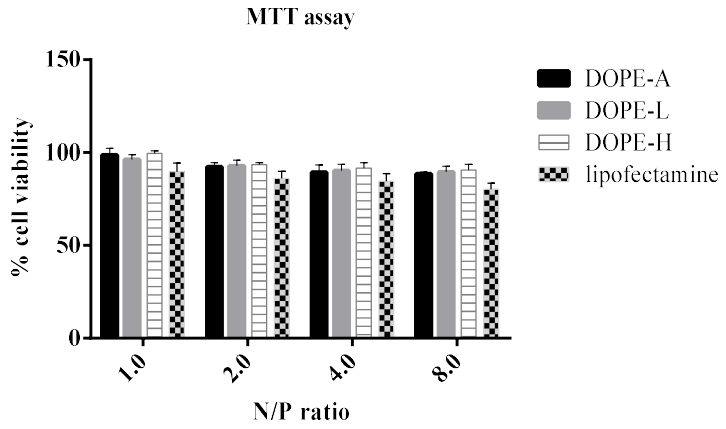

Figure 5. 33 % Cell viability at various L/P ratio for modified lipoplex formulations

Toxicity of most currently available cationic lipids is a limiting factor in their practical uses. We have compared the toxicity of the synthesised lipids and of the array of commercially available cationic lipids, in combination with DNA for the cultured cells. This study showed that the synthesised monocationic lipids have no detectable toxicity in the studied range of concentrations efficient for gene delivery, this property found, again, in their polycationic counterpart, DOTAP, and not generally expected in a monocationic lipids. The another reason for their non-cytotoxic behaviour is that they are capable of being degraded in the living cells into non-toxic, metabolizable fragments comprising (1) a guanidino domain for arginine, leucine and ammonium domain for histidine as a bearer of the cationic charge; (2) a hydrophobic domain capable of causing the molecule to form vesicular structures in aqueous medium and (3) a hydrophilic arm linking together the above two domains.

5.7.13 Cellular uptake study

Confocal microscopy images of the cell uptake studies are shown in figure 5.34. Each image depicts the cellular uptake of developed DOPE modified lipoplexes against the naked DNA and Lipofectamine-2000 for comparison. As it can be seen in figure, there wasn't any visible expression seen in case of the naked eGFP while all other formulations showed extensive eGFP expression as indicated by intense green fluorescence from the cells. Highest fluorescence was seen with lipoplex formulated with arginine modified DOPE in comparison to lipoplex formulated from leucine, histidine modified DOPE and lipofectamine-2000. Improved buffering capacities of modified DOPE as well as the effective escape of the liposomes which would be provided by the DOPE. Furthermore, increased head-group size in synthesised lipids would provide better membrane destabilization after complete ionization of the lipids, leading to release of cDNA inside the cytosol. Similar explanations can also be expanded to cDNA solution and lipofectamine-2000 that there will not be enough buffering capacity leading to diminish cellular uptakes. In addition, macropinocytisis and rearrangement of actin cytoskeleton play an important part in arginine mediated uptake of nano career. This mechanisms played important part in improved uptake of DOPE-A with compared to other lipoplexes and naked cDNA formulation.

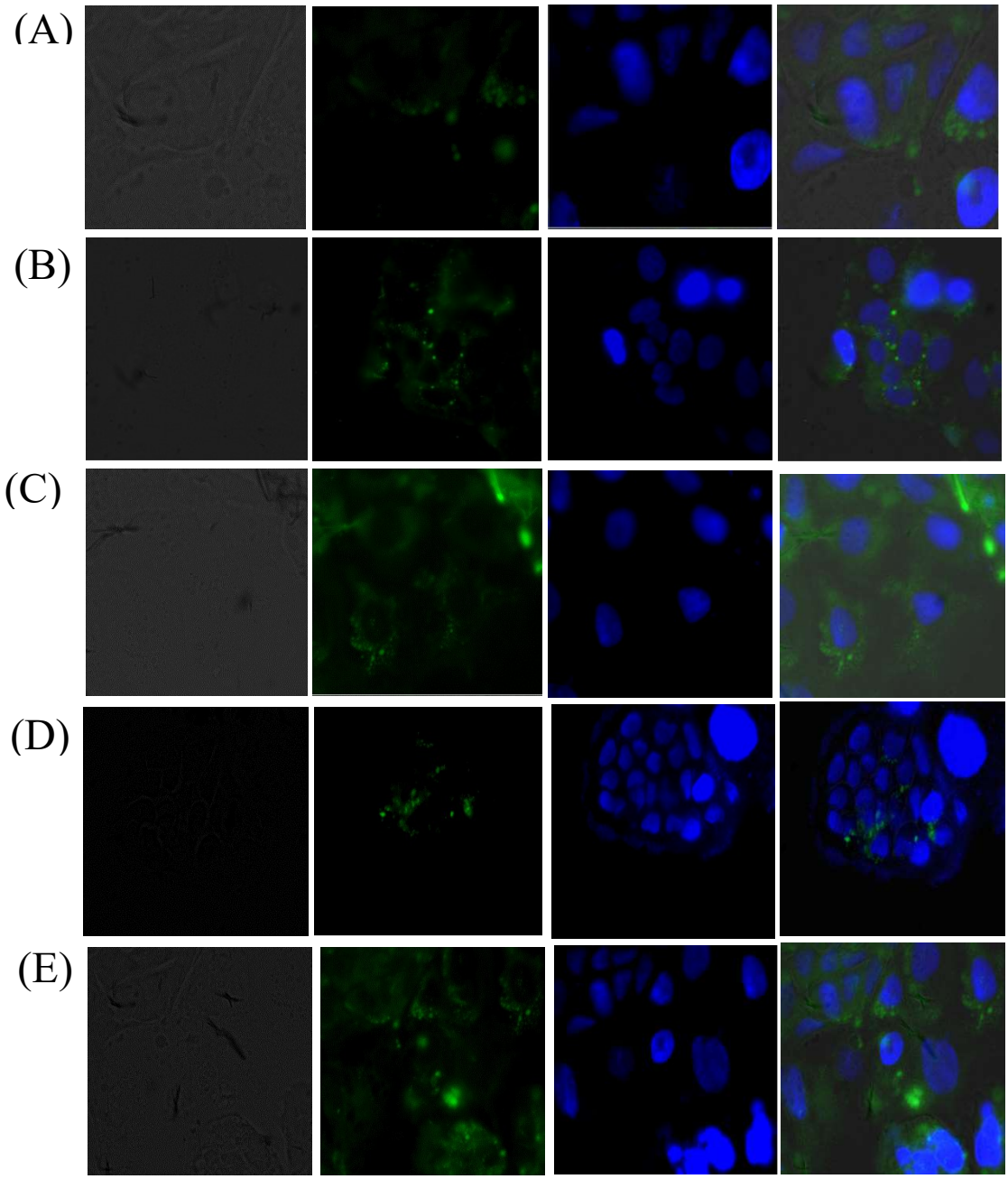

Figure 5. 34 Cellular uptake of following formulations (A) DOPE-H, (B) DOPE-L, (C) DOPE-A, (D) naked DNA and (E) Lipofectamine-2000

5.7.14 Cell permeation study

Cells were seeded at a density of 1,00,000 cells/cm^2 onto 6-well transwell plates with an insert area of 4.6 cm^2 and a the polycarbonate membrane of 0.45 µm pore size. Culture medium was changed alternate day and permeation study was actually initiated after 21 days post seeding. Naked cDNA, liposomes formulated from modified lipids and lipofectamine-2000 were added in the apical compartment. TEER values of the cell monolayer was measured, both before commencing and after completing the permeation experiment. Only data derived from experiments with final TEER values exceeding 80% of the initial values was used. Permeation of formulations across the cell monolayer was monitored by sampling the solutions in receiver compartments, at predefined time points for the duration of 4h. Samples of 20 µl were drawn after 15, 30, 60, 90, 120, 180 and 240 min. The withdrawn samples were replaced by freshly prepared media.

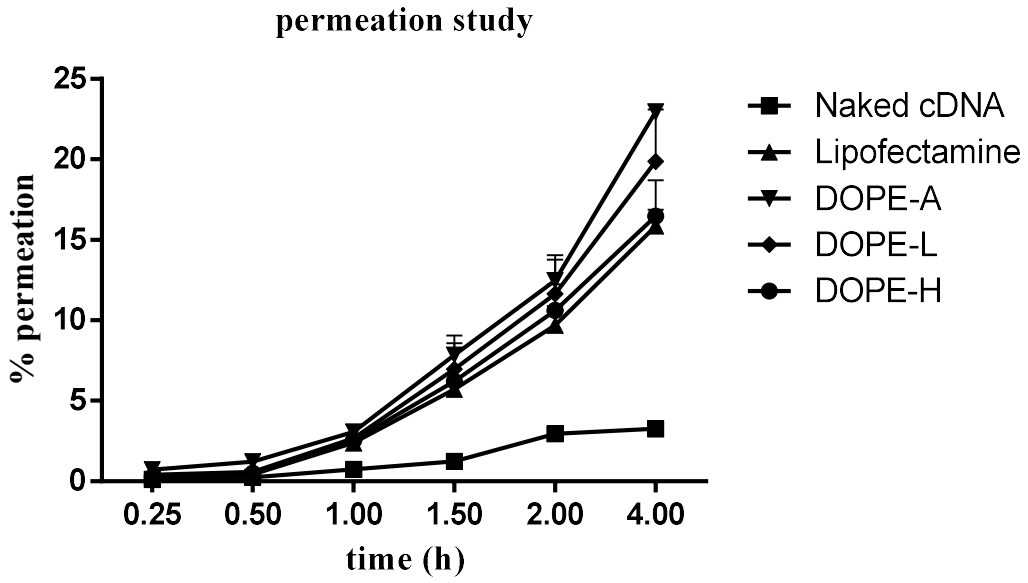

Figure 5. 35 Graph of cell permeation ability of lipoplex formulation through SHSY5Y cell line

Results shown in figure 5.35 backs the results obtained from cell uptake studies. As with the confocal study, % permeation of lipoplex formulated from arginine modified lipoplex was maximum in comparison to lipoplex formulated from leucine and histidine modified DOPE, lipofectamine-2000 and naked cDNA.

5.7.15 Western blot analysis

Reduced level of p11 protein level in SHSY5Y cells by INF was detected using western blot with visible bands as shown in figure 5.36. Compared to the protein level in treatment with PBS (control), treatment with INF (disease control) showed significant decrease in p11 protein, around 52 % reduced level of p11 in disease control cells in comparison to cells treated with PBS and cells treated with lipoplex formulated from amino acids modified DOPE showed increase in the level of p11 protein as compared to disease control cells. More specifically, cells treated with DOPE-A showed around 46 % rise in p11 protein level, DOPE-L showed 36 % upsurge and DOPE-H showed 28 % increase in the p11 protein level in comparison to disease control cell protein level. Lipoplex formulated with DOPE-A clearly showed more difference with protein level in comparison to other formulations.

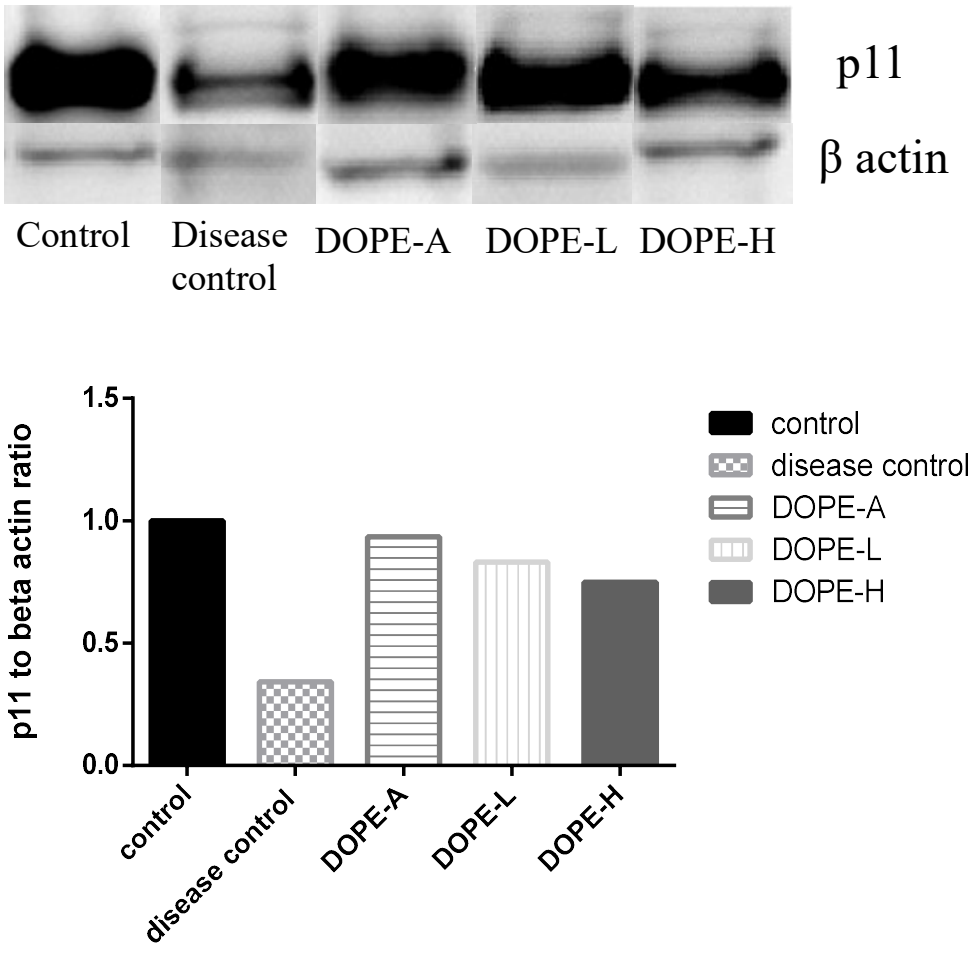

Figure 5. 36 Western blot analysis of p11 protein in cells and correlated graph

5.7.16 RT-PCR

The RT-PCR results in table 5.23 and figure 5.37 demonstrated that after treatment with interferon, p11 mRNA level significantly reduced in comparison to mRNA level of cells treated with PBS. Interferon downregulates the level of p11 in SHSY5Y cells which also justified the role of interferon in inducing depression by downregulating p11 level. After treatment with DOPE modified liposomal formulations, trend observed in gene transfection efficiency was in concordance with the results of western blot analysis. Results showed that liposomal formulation increased gene expression in disease control cells, more effectively than naked cDNA formulation. All liposomal formulation contain lipid DOPE, which explained its increased interaction between formulations and bio-membranes due to their structure resemblance and membrane fusing properties. Moreover, DOPE modifications with different amino acids, increased its fusing property as well as endosomal escape. Among the modifications, arginine modified DOPE had maximum buffering capacity as well permeation capacity resulting in maximum intracellular cDNA delivery resulting in increased gene expression which results in increased protein level as shown with western blot analysis which was proved in study depicted above.

Table 5. 23 % Gene expression in SHSY5Y cells after treatment with interferon, naked DNA and lipoplex formulations

Formulations	Gene expression (%)
PBS	100 ± 1.61
interferon	39.8 ± 3.15
naked cDNA	51.72 ± 3.24
DOPE-A	85.41 ± 4.12
DOPE-L	69.15 ± 3.46
DOPE-H	61.97 ± 3.72

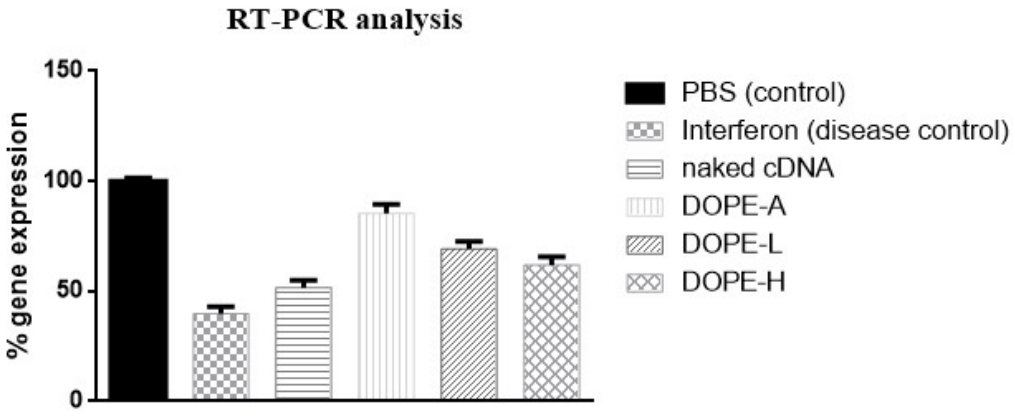

Figure 5. 37 mRNA level in cells treated with interferon, naked DNA and modified liposomes

References

1. Zhang Y, Satterlee A, Huang L. In vivo gene delivery by nonviral vectors: overcoming hurdles? Molecular therapy. 2012;20(7):1298-304.

2. Mayet N, Choonara YE, Kumar P, Tomar LK, Tyagi C, Du Toit LC, et al. A comprehensive review of advanced biopolymeric wound healing systems. Journal of pharmaceutical sciences. 2014;103(8):2211-30.

3. Kabanov AV, Eisenberg A, Kabanov VA. Composition for delivery of biological agents and methods for the preparation thereof. Google Patents; 2007.

4. Lomas H, Du J, Canton I, Madsen J, Warren N, Armes SP, et al. Efficient Encapsulation of Plasmid DNA in pH-Sensitive PMPC–PDPA Polymersomes: Study of the Effect of PDPA Block Length on Copolymer–DNA Binding Affinity. Macromolecular bioscience. 2010;10(5):513-30.

5. Davidsen J, Rosenkrands I, Christensen D, Vangala A, Kirby D, Perrie Y, et al. Characterization of cationic liposomes based on dimethyldioctadecylammonium and synthetic cord factor from M. tuberculosis (trehalose 6, 6′-dibehenate)—a novel adjuvant inducing both strong CMI and antibody responses. Biochimica et Biophysica Acta (BBA)-Biomembranes. 2005;1718(1):22-31.

6. Gokhale PC, Zhang C, Newsome JT, Pei J, Ahmad I, Rahman A, et al. Pharmacokinetics, toxicity, and efficacy of ends-modified raf antisense oligodeoxyribonucleotide encapsulated in a novel cationic liposome. Clinical cancer research. 2002;8(11):3611-21.

7. Gustafsson J, Arvidson G, Karlsson G, Almgren M. Complexes between cationic liposomes and DNA visualized by cryo-TEM. Biochimica et Biophysica Acta (BBA)-Biomembranes. 1995;1235(2):305-12.

8. Geall AJ, Blagbrough IS. Rapid and sensitive ethidium bromide fluorescence quenching assay of polyamine conjugate–DNA interactions for the analysis of lipoplex formation in gene therapy. Journal of pharmaceutical and biomedical analysis. 2000;22(5):849-59.

9. Hyvönen Z, Hämäläinen V, Ruponen M, Lucas B, Rejman J, Vercauteren D, et al. Elucidating the pre-and post-nuclear intracellular processing of 1, 4-dihydropyridine based gene delivery carriers. Journal of controlled release. 2012;162(1):167-75.

10. Palla B, Shah D. Stabilization of high ionic strength slurries using surfactant mixtures: molecular factors that determine optimal stability. Journal of colloid and interface science. 2002;256(1):143-52.

11. Daly E, Saunders BR. A study of the effect of electrolyte on the swelling and stability of poly (N-isopropylacrylamide) microgel dispersions. Langmuir. 2000;16(13):5546-52.

12. Lee S-Y, Huh MS, Lee S, Lee SJ, Chung H, Park JH, et al. Stability and cellular uptake of polymerized siRNA (poly-siRNA)/polyethylenimine (PEI) complexes for efficient gene silencing. Journal of Controlled Release. 2010;141(3):339-46.

13. de Lima MCP, Simoes S, Pires P, Faneca H, Düzgüneş N. Cationic lipid–DNA complexes in gene delivery: from biophysics to biological applications. Advanced drug delivery reviews. 2001;47(2-3):277-94.

14. Zhang Y, Anchordoquy TJ. The role of lipid charge density in the serum stability of cationic lipid/DNA complexes. Biochimica et Biophysica Acta (BBA)-Biomembranes. 2004;1663(1):143-57.

15. Lopez JA, Chen J, Sun S, Zheng Y, Delaney M, Capocelli KE, et al., editors. An in vitro system for microvessel assembly and its use for the study the biology of the microvasculature and the blood. ANGIOGENESIS; 2014: SPRINGER VAN GODEWIJCKSTRAAT 30, 3311 GZ DORDRECHT, NETHERLANDS.

16. Kyriakides TR, Cheung CY, Murthy N, Bornstein P, Stayton PS, Hoffman AS. pH-sensitive polymers that enhance intracellular drug delivery in vivo. Journal of Controlled Release. 2002;78(1-3):295-303.

17. Lv H, Zhang S, Wang B, Cui S, Yan J. Toxicity of cationic lipids and cationic polymers in gene delivery. Journal of Controlled Release. 2006;114(1):100-9.

18. Rothen-Rutishauser BM, Schürch S, Haenni B, Kapp N, Gehr P. Interaction of fine particles and nanoparticles with red blood cells visualized with advanced microscopic techniques. Environmental science & technology. 2006;40(14):4353-9.

19. Wightman L, Kircheis R, Rössler V, Carotta S, Ruzicka R, Kursa M, et al. Different behavior of branched and linear polyethylenimine for gene delivery in vitro and in vivo. The journal of gene medicine. 2001;3(4):362-72.

20. Quent V, Loessner D, Friis T, Reichert JC, Hutmacher DW. Discrepancies between metabolic activity and DNA content as tool to assess cell proliferation in cancer research. Journal of cellular and molecular medicine. 2010;14(4):1003-13.

21. Plumb JA, Milroy R, Kaye S. Effects of the pH dependence of 3-(4, 5-dimethylthiazol-2-yl)-2, 5-diphenyltetrazolium bromide-formazan absorption on chemosensitivity determined by a novel tetrazolium-based assay. Cancer research. 1989;49(16):4435-40.

22. Fischer RS, Wu Y, Kanchanawong P, Shroff H, Waterman CM. Microscopy in 3D: a biologist's toolbox. Trends in cell biology. 2011;21(12):682-91.

23. Paddock SW. Principles and practices of laser scanning confocal microscopy. Molecular biotechnology. 2000;16(2):127-49.

24. Srinivasan C, Burgess DJ. Optimization and characterization of anionic lipoplexes for gene delivery. Journal of Controlled Release. 2009;136(1):62-70.

25. Toimela T, Mäenpää H, Mannerström M, Tähti H. Development of an in vitro blood–brain barrier model—cytotoxicity of mercury and aluminum. Toxicology and applied pharmacology. 2004;195(1):73-82.

26. Paradis A, Leblanc D, Dumais N. Optimization of an in vitro human blood–brain barrier model: Application to blood monocyte transmigration assays. MethodsX. 2016;3:25-34.

27. Moreno FJ, Rubio LA, Olano A, Clemente A. Uptake of 2S albumin allergens, Ber e 1 and Ses i 1, across human intestinal epithelial Caco-2 cell monolayers. Journal of agricultural and food chemistry. 2006;54(22):8631-9.

28. Aggarwal P, Hall JB, McLeland CB, Dobrovolskaia MA, McNeil SE. Nanoparticle interaction with plasma proteins as it relates to particle biodistribution, biocompatibility and therapeutic efficacy. Advanced drug delivery reviews. 2009;61(6):428-37.

29. Moylan S, Maes M, Wray N, Berk M. The neuroprogressive nature of major depressive disorder: pathways to disease evolution and resistance, and therapeutic implications. Molecular psychiatry. 2013;18(5):595.

30. Ozsolak F, Milos PM. RNA sequencing: advances, challenges and opportunities. Nature reviews genetics. 2011;12(2):87.

31. Geng S, Yang B, Wang G, Qin G, Wada S, Wang J-Y. Two cholesterol derivative-based PEGylated liposomes as drug delivery system, study on pharmacokinetics and drug delivery to retina. Nanotechnology. 2014;25(27):275103.

32. Wilschut J, Corver J, Nieva JL, Bron R, Moesby L, Reddy KC, et al. Fusion of Semliki Forest virus with cholesterol-containing liposomes at low pH: a specific requirement for sphingolipids. Molecular membrane biology. 1995;12(1):143-9.

33. Lee AG. How lipids affect the activities of integral membrane proteins. Biochimica et Biophysica Acta (BBA)-Biomembranes. 2004;1666(1):62-87.

34. Jimbo T, Sakuma Y, Urakami N, Ziherl P, Imai M. Role of Inverse-Cone-Shape Lipids in Temperature-Controlled Self-Reproduction of Binary Vesicles. Biophysical Journal. 2016;110(7):1551-62.

35. Bemporad D, Luttmann C, Essex J. Behaviour of small solutes and large drugs in a lipid bilayer from computer simulations. Biochimica et Biophysica Acta (BBA)-Biomembranes. 2005;1718(1):1-21.

36. Srivastava R, Sahney R, Upadhyay S, Gupta R. Membrane permeability based cholesterol sensor—A new possibility. Journal of Membrane Science. 2000;164(1-2):45-9.

37. Di Russo NV, Estrin DA, Martí MA, Roitberg AE. pH-Dependent Conformational Changes in Proteins and Their Effect on Experimental pK(a)s: The Case of Nitrophorin 4. PLoS Computational Biology. 2012;8(11):e1002761.

38. Loomis K, McNeeley K, Bellamkonda RV. Nanoparticles with targeting, triggered release, and imaging functionality for cancer applications. Soft Matter. 2011;7(3):839-56.

39. Guo X, Szoka F. Steric stabilization of fusogenic liposomes by a low-pH sensitive PEG− diortho ester− lipid conjugate. Bioconjugate chemistry. 2001;12(2):291-300.

40. Muhl L, Galuska SP, Öörni K, Hernández-Ruiz L, Andrei-Selmer LC, Geyer R, et al. High negative charge-to-size ratio in polyphosphates and heparin regulates factor VII-activating protease. The FEBS journal. 2009;276(17):4828-39.

41. Boyle WS, Senger K, Tolar J, Reineke TM. Heparin enhances transfection in concert with a trehalose-based polycation with challenging cell types. Biomacromolecules. 2016;18(1):56-67.

42. Bondi ML, Azzolina A, Craparo EF, Lampiasi N, Capuano G, Giammona G, et al. Novel cationic solid-lipid nanoparticles as non-viral vectors for gene delivery. Journal of Drug Targeting. 2007;15(4):295-301.

43. Liu Z, Zhang Z, Zhou C, Jiao Y. Hydrophobic modifications of cationic polymers for gene delivery. Progress in Polymer Science. 2010;35(9):1144-62.

44. Kim J-M, Shin E, Ryou S-M, Yeom J-H, Lee K. Gene delivery platforms. Biotechnology and bioprocess engineering. 2013;18(4):637-47.